A Cognitive Sensing Algorithm for Coexistence Scenarios with LTE

Peyman Karimzadeh Reghbati

A Thesis
In the Department
of
Electrical and Computer Engineering

Presented in Partial Fulfillment of the Requirements
For the Degree of Master of Applied Science
Concordia University
Montréal, Québec, Canada

December 2014

Concordia University

School of Graduate Studies

This is to certify that the thesis prepared

By: **Peyman Karimzadeh Reghbati**

Entitled: **A Cognitive Sensing Algorithm for Coexistence Scenarios with LTE**

and submitted in partial fulfillment of the requirements for the degree of

Master of Applied Science (Electrical and Computer Engineering)

complies with the regulations of the University and meets the accepted standards with respect to originality and quality.

Signed by the final examining committee:

_____ Chair
Dr. M. Z. Kabir

_____ Examiner, External to the Program
Dr. C. Assi (CIISE)

_____ Examiner
Dr. Y. R. Shayan

_____ Thesis Supervisor
Dr. M.R. Soleymani

Approved by _____
Dr. W. E. Lynch, Chair
Department of Electrical and Computer Engineering

December 2014

_____
Dr. Amir Asif, Dean
Faculty of Engineering and Computer Science

Abstract

A Cognitive Sensing Algorithm for Coexistence Scenarios with LTE

Peyman Karimzadeh Reghbati
Concordia University, 2014

Increasing demand for high data rate wireless communication motivates the wireless engineers to develop advanced technologies to address such needs. LTE and LTE-Advanced are examples of such wireless technologies, which support high data rate and a large number of users. However, higher data rate communication requires more frequency bandwidth.

Recent studies have shown that the inefficient utilization of frequency spectrum is one of the main reasons for the scarcity of frequency bandwidth. Cognitive Radio Network is introduced as a promising solution for this problem. It increases the utilization of bandwidth, by intelligently sensing the channel environment and dynamically providing access to the available resources (frequency bands) for a secondary user.

In this thesis, we developed an algorithm for dynamically detecting and anticipating the existence of underutilized resources in LTE system. The algorithm should be a real-time operation, i.e. the decision on availability of a detected resource should be made within a time much less than scheduling update period of LTE. This is the only way that rest of the unused resources becomes usable. For each specific channel assignment, the algorithm requires to start sensing as soon as possible.

Therefore, we develop the algorithm in three main steps. The first step is to blindly detect and identify the LTE-Downlink signal using cyclostationarity property of OFDM scheme. The second step is the acquisition of the LTE-Downlink sub-frame timing, which is basically performed by detecting the Primary Synchronization Signal. The third step is to detect unused resources, for the duration of their transmission. This step is using a frequency domain energy detector. By performing the first and second steps, the sub-frame timing and scheduling update instances are known. So basically the algorithm does not require any previous knowledge of the LTE signal.

We evaluate the performance of the proposed algorithm with respect to the tolerable amount of interference at the primary user side. Using the proposed algorithm, in average up to 81 % of unused resources can be used by the secondary user.

To my parents, my sister,
and specially my lovely wife, Sheida.

Acknowledgments

First and foremost, I would like to express my gratitude to my supervisor, Professor M. Reza Soleymani, for giving me the opportunity to work in his group and for his support and encouragement throughout my research not only as a professor but also as a friend. Without his guidance and instruction, I would have not been able to complete this work.

I would like to thank all members of my Master defense committee: Prof. Amir Asif, Prof. William E. Lynch, Prof. Yousef R. Shayan ,Prof. C. Assi and Dr. M. Z. Kabir. I appreciate their valuable comments and all the time they spent reading this thesis.

I also want to thank all current and previous members of the Wireless and Satellite Communications Laboratory for their help and support, especially Mr. Khoshneviss. In addition, I wish to thank NSERC CRD as well as InterDigital Canada Ltd. and PROMPT. More than anyone else, I would like to thank my parents, Yasamin and Akbar. I would not be where I am today without their love, encouragement and unlimited sacrifices. I only hope I have made their support worthwhile. My thanks also go to my beloved sister, Dr. Fereshteh Karimzadeh, for her support. Finally, I express my appreciation to my wife, Sheida Banasaz, for all her support, in particular the comfortable home atmosphere that is the result of her work.

Contents

List of Figures

List of Tables

List of Abbreviation

PSS	Primary Synchronization Signal
SSS	Secondary Synchronization Signal
BW	Bandwidth
LTE	Long Term Evolution
LTE-A	LTE- Advanced
4G	Fourth Generation
CR	Cognitive Radio
CRN	Cognitive Radio Network
FDD	Frequency Division Duplex
DL	Down Link
SDR	Software Defined Radio
VoIP	Voice Over Internet Protocol
RF	Radio Frequency
FPGA	Field Programmable Gate Arrays
DSP	Digital Signal Processors
GPP	General Purpose Processors
FCC	Federal Communications Commission
DSA	Dynamic Spectrum Access
SU	Secondary User
PU	Primary User
SNR	Signal to Noise Ratio
SINR	Signal to Interference and Noise Ratio
UWB	Ultra WideBand
3GPP	3rd Generation Partnership Project
MAC	Media Access Control
DL-SCH	Down Link Shared Channel
OFDM	Orthogonal Frequency Division Multiplexing
ISI	Inter-Symbol-Interference
IFFT	Inverse Fast Fourier Transform
IDFT	Inverse Discrete Fourier Transform
FFT	Fast Fourier Transform
CP	Cyclic-Prefix
AMC	Adaptive Modulation and Coding
QPSK	Quadrature Phase Shift Keying
QAM	Quadrature Amplitude Modulation

CQI	Channel Quality Indicator
AWGN	Additive White Gaussian Noise
RB	Resource Block
RBP	Resource Block Pair
RE	Resource Element
CC	Component Carrier
PHY	Physical Layer
ZC	Zadoff-Chu Sequence
DC	Direct Current
SHD	Spectrum Hole Detector
CAF	Cyclic Autocorrelation Function
CFAR	Constant False Alaram Rate
GFLOPS	Giga Floating Point per Second
ROC	Region of Coherent
LLR	Log Likelihood Ratio
ED	Energy Detector
PSD	Power Spectral Density
CDMA	Code Division Multiple Access
BER	Bit Error Rate
NC-OFDM	Non-Continguous OFDM
UE	User Equipment

List of Symbols

α	Cyclic Frequency (CH3)
β	Activity Factor of PU
γ	Normalized Threshold level
η	Radio Link Bandwidth Utilization
λ	Wave Length
$\Gamma_u(.)$	Upper Incomplete Gamma Function
σ_z	Gaussian noise standard deviation
Δf	OFDM Subcarrier Spacing
τ	Time shift in Auto-correlation Function
$\delta(.)$	Dirac Delta Function
S	Signal Power (CH1)
N	Noise Power (CH1)
C	Channel capacity
E_b	Energy per bit
E_s	Energy per symbol
R_b	Bit Rate
N_o	Noise Power Density
a_k	M-QAM symbols
N_c	Total number of active sub-carriers within LTE-DL OFDM
k	Sub-carrier Index
l	OFDM Symbol Index within a sub-frame
M	Number of Signal levels, Modulation order
$s(n)$	Base-band OFDM Signal Sample
n	sampling index in time
T_s	Sampling time period
T_{symb}	OFDM symbol Duration
T_u	Useful OFDM Symbol Duration
T_{CP}	Cyclic-Prefix Length also known as T_g
$d_u(n)$	Root u ZC sequence samples
$y(t)$	Received Signal
$w(t)$	White Gaussian Noise added to OFDM signal
$s(t)$	OFDM Transmitted Signal
$R_x(.,.)$	Autocorrelation Function of the observed signal x
$R_x^\alpha(.)$	Cyclic Autocorrelation Function of x
r_u	Generated Replica for detecting the PSS sequence

$Q_u(n)$	Magnitudes of Cross Correlation of R_u and an OFDM symbol
R_u	Generated Replica for detecting the OFDM symbol Containing PSS
$ZC_u^L(n)$	Length L, Root u, Zadoff-Chu Sequence
N_{ZC}	Length of the ZC Sequence
P_{miss}	Probability of Miss Detection
q	Probability of Interference due to miss detection
P_{FA}	Probability of False Alarm
P_{HD}	Probability of detecting the Spectrum Hole correctly
L	Length of a sequence or series of data
$N_{ifft/fft}$	Number of points in IFFT/FFT process
N_{RB}	Total Number of Resource Blocks
$z(k)$	White Gaussian Noise added to M-QAM symbols
N_{sc}^{RB}	Number of sub-carriers per Resource Block
N_{sc}	Number of sub-carrier in LTE-DL OFDM signal $N_{sc} = N_{sc}^{RB} \times N_{RB}$
Q_n	Macum Q Function (CH4)
μ	Non-Centrality Parameter
P_I	Probability of Interference per Resource Block
N_{symb}	Number OFDM Symbol per subframe
β	Primary User Activation factor
R_{PU}^{RBP}	Primary user Data-Rate per RBP
R_{SU}^{RBP}	Secondary user Data-Rate per RBP
R_{PU}^{Loss}	Primary user Data-Rate Loss
R_{SU}	Secondary user Data-Rate Gained

Chapter 1

Introduction

In this work we developed a multi-step algorithm to sense the occupancy of the time-frequency resource grids of an LTE or an LTE-Advanced Downlink signal, in a real-time manner. The secondary user of the system uses this algorithm to dynamically find and occupy the unused spectrum for a specific duration. As the scheduling process in LTE is performed every one millisecond, unused frequency spectrum will not last more than this duration. Therefore, the whole sensing and reusing procedure of detected spectrum should be done within this period. That is why the sensing process requires accurate sub-frame timing information of the LTE signal. Acquisition of the sub-frame timing is done as the first task, by detecting the Synchronization Sequence within LTE-Downlink signal. The next task is to sense the beginning of each sub-frame. This process has to be done very fast, in order to provide more communication time for secondary users. Otherwise the sensed resources are either passed, or the remaining time is not useful for any secondary purposes.

In this chapter, we first discuss Spectrum Scarcity and Low Bandwidth Utilization. Many studies have been done in this respect, and some of them are presented here. We also present an overview of the proposed algorithm, followed by contribution of the thesis. Thesis Outline terminates this chapter.

1.1 Problem Statement

With the advances in technology, powerful portable devices are designed. These devices support many applications, which require high quality and high rate wireless communication links. Wireless service providers are always looking for ways to satisfy the users. Due to the increasing demand for higher data rates, they are interested in systems, that supports high data rate and a large number of users. However, higher data rate requires higher bandwidth, which is an expensive wireless resource. So, one resolution is to increase the bandwidth efficiency of the system as much as possible.

LTE is the first global wireless standard, which is designed to support high data rate, and a large number of users. Although such technologies are very well designed, there is a drawback in bandwidth utilization. The users at the edge of a cell may experience low quality of service, which leads to low bandwidth efficiency. This drawback is not only considerable for an LTE system, but also traceable in any other system which suffer from imperfect handover, while support high mobility.

In addition to the stated issue, non-uniform distribution of service demand during 24 hours, and 7 days of a week decreases the utilization of frequency spectrum. This is also another waste that could be prevented.

Cognitive Radio Networks provide a promising solution for reducing underutilized frequency spectrum. It allows an unlicensed user to access a licensed bandwidth under certain conditions. As an example, the amount of interference, that the unlicensed user may produce for the licensed one, should not exceed a certain level.
We leave the concept of cognitive radio for Chapter 2, and provide more details for presented concerns.

1.1.1 Spectrum Scarcity

The growing demand for mobile applications applied to today's telecommunication industry, leads to increasing request for more regulation and standardization of spectrum usage. The radio spectrum is rapidly becoming one of our planet's most valuable resources. A relatively small portions of this commodity, costs billions of U.S. dollars [2]. In "Ericsson Mobility Report", June 2014, it is indicated that the number of smart-phone subscriptions will increase to more than 5.6 billion, while this was 1.9 billion in 2013 [3]. Associated with this, the data traffic growth is almost 65% from 2013 to 2014, while the voice traffic has almost constant value during last 4 years. The Internet traffic, particularly due to video is seen as the major component of this growth. The ever growing need for higher data rate wireless communication requires more frequency bandwidth.

1.1.2 Bandwidth Utilization

Recent studies have shown that the spectrum scarcity is derived more from inefficient usage rather than unavailability [4], [5]. Achieving high data rate with high bandwidth efficiency is an important challenge in this respect. Fortunately, there is a direct correlation between allocated bandwidth and the achievable data rate that a channel can support. For example, in its simplest form, this is described by the Nyquist bandwidth formula:

$$R = 2B \ (for\ binary\ signals) \tag{1.1}$$

where R is the transmission rate in bits per second, and B is the bandwidth in Hertz. In general, for the M-ary transmission R is the baud (or symbol rate).

In 1948, Shannon provided the basic theoretical tools needed to determine the maximum rate, also known as the channel capacity, by which information can be transferred over a given communication channel [6]. Although relatively complicated

in the general case, for the special case of communication over a channel, for example a radio link, only impaired by additive white Gaussian noise, the channel capacity C is given by the relatively simple expression [7]:

$$C = B.log_2(1 + \frac{S}{N}) \quad bits/second \tag{1.2}$$

where again B is the bandwidth available for the communication, S denotes the received signal power, and N denotes the power of the white noise impairing the received signal.

The above equation clearly depicts the two fundamental factors which are limiting the achievable data rate: The received signal power, and the available bandwidth. Thus, the relationship between the available bandwidth and the transmission data rate is so close. In other words, if we assume a fixed signal to noise ratio, we need to use a certain amount of bandwidth to be able to achieve a certain amount of transmission rate. This simply shows the restriction boundaries in a wireless communication system. Clearly, the information rate can never exceed the channel capacity. Together with above expressions for the received signal power and noise power, this leads to the inequality:

$$R \leqslant C = B. \log_2 (1 + \frac{S}{N}) = B. \log_2 (1 + \frac{E_b.R_b}{N_o.B}) \tag{1.3}$$

or, by defining the radio-link bandwidth utilization $\eta = R_b/B$,

$$\eta \leqslant \log_2 (1 + \eta.\frac{E_b}{N_o}) \quad bits/sec./Hz \tag{1.4}$$

where E_b is the average received energy per bit, N_o is the power spectral density of the noise, and R_b is bit-rate. This inequality can be reformulated to provide a lower bound on the required received energy per information bit, normalized to the noise

power density, for a given bandwidth utilization η:

$$\frac{E_b}{N_o} \geqslant min\,\{\frac{E_b}{N_o}\} = \frac{2^\eta - 1}{\eta} \tag{1.5}$$

The rightmost expression is the minimum required E_b/N_o at the receiver as a function of the bandwidth utilization.

As was mentioned, one way to have better bandwidth utilization (having higher data rate on a fixed bandwidth), is to have higher E_b/N_o. This has been the major effort of many researchers and developers during last 20 years. There were vast improvements in design and implementation of wireless transmitters and receivers to have a better signal to noise ratio at the receiver side. From different channel coding schemes to data compression methods, advanced modulation scheme to single or multi-carrier transmission modes, they are all invented and exploited to make high data rate transmission possible with the acceptable bandwidth utilization. The relation between bandwidth utilization and $\left(E_b/N_o\right)_{req}$ is shown in figure 1.1. For Further reading in this vast topic please refer to [7], [8], [9], and [10].

In the next section we will introduce another approach for increasing the bandwidth utilization. In the last decade, there have been many studies regarding the spectrum occupancy measurements in different areas. The spectrum occupancy was defined to be the fraction measured in time and frequency where the signal strength exceeds a specific threshold [5]. The results of those studies show that significant spectrum is available in most bands, meaning that currently the frequency spectrum is underutilized. The maximum average spectrum occupancy was found to be 13.1% in New York City [11]. Then, by sensing the availability of the user who owns the spectrum (licensed user), a secondary user (unlicensed user) is able to occupy the spectrum only if it causes no interference for the main user. This is basically the concept of Cognitive Radio Networks, which will be provided in detail.

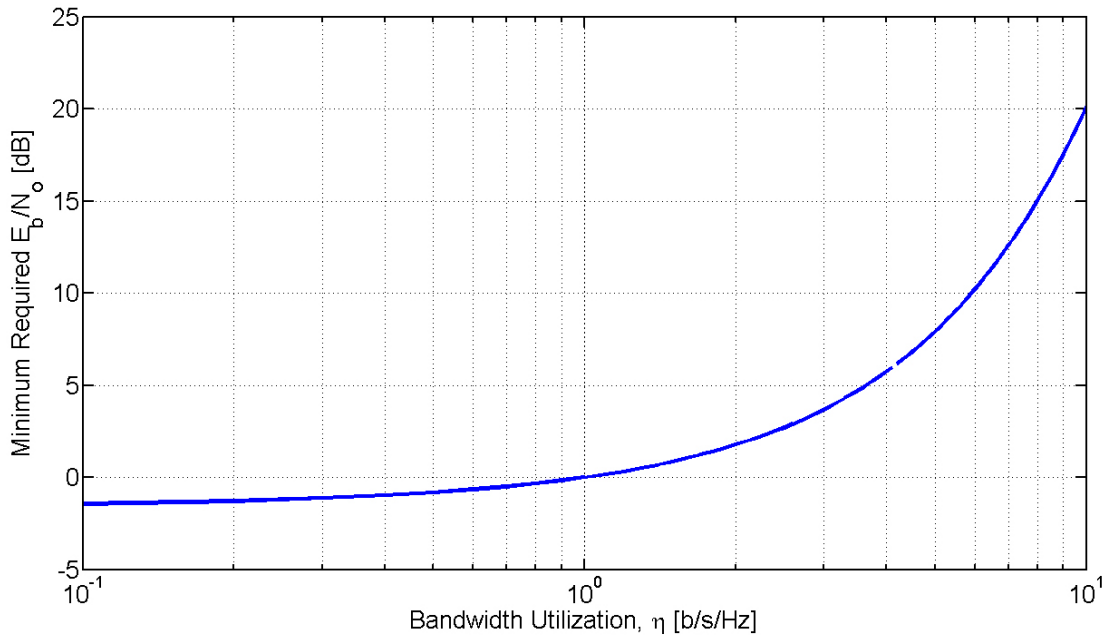

Figure 1.1: Minimum required E_b/N_o at the receiver side as a function of bandwidth utilization $b/s/Hz$

1.2 Possible Solution

Many attempts have been done during last decades to address the stated issues. Technologies such as WiMAX and LTE/ LTE-Advanced, have been designed to support high data rate and a large number of users. However, high mobility devices located at the edge of a cell may experience degraded service levels. Limited possibilities to reconfigure networks and terminals depending on spectrum availability is the main reason for that [11]. Accordingly, these limitations of 4G systems, often referred to 4G bottlenecks, are expected to become the major issue for Quality of Service in the future.

Considering the above discussion, following two statements describe the fundamental of this thesis:

1. With recent developments in Cognitive Radio technology, it is now possible for these systems to simultaneously respect the rights of incumbent license holders

while providing additional flexible access to spectrum.

2. The ability to sense, and identify the spectrum holes within the operating frequency band of primary user (say LTE system) is a possible solution for increasing the bandwidth utilization.

Thus our solution is to identify and sense the LTE-DL signal, and dynamically find underutilized portion of operating frequency band within LTE Downlink. We refer the term ***cognitive sensing*** to the proposed algorithm.

The secondary user for such a Cognitive Sensing algorithm could be any wireless system which is able to configure its transmission signal according to the detected available time-frequency resources. For example Non-contiguous OFDM transmission Scheme is a good candidate for that, as it is described in Chapter 5.

1.3 Contribution of the Thesis

In this thesis, we propose a combined algorithm for Cognitive Sensing under certain assumptions. We assume that the primary user of the cognitive network is an LTE or LTE Advanced system that operates in Frequency-Division-Duplex (FDD) mode. Thus the licensed frequency band, which is going to be shared based on its availability, is LTE Downlink frequency band. Therefore, the contributions of the thesis are:

1. LTE Dynamic Spectrum Sensing
    - Combined method for blind detection and identification of primary signal, and finding its frame timing.
    - Sensing and anticipating the spectrum holes within LTE-DL frame.
2. Overal System Evaluation
    - Average data rate achieved by secondary user, and the average primary data rate lost due to interference caused by secondary user.

- Bandwidth Utilization of the overall system.

1.4 Thesis Outline

The thesis is organized as follow: In Chapter 2 we cover the required background material. For example, definition and organization of the Cognitive Radio Networks are provided, as well as required parts of LTE/ LTE-A systems specifications. The literature review of the work also presented in Chapter 2. Chapter 3, consists of the proposed algorithm for acquisition of primary user signal timing. This is a pre-requisite step for the cognitive sensing and also secondary user transmission. We propose a Dynamic Spectrum Hole Detector based on frequency domain energy detection in Chapter 4. The algorithm should be fast and accurate as it is going to sense the ongoing LTE-DL sub-frame. Chapter 5 suggests a transmission algorithm which fits to the proposed cognitive sensing. The average lost data rate due to the interference is calculated. The expected achievable data rate for secondary user is also calculated. The overall improvement in bandwidth utilization is depicted as well. Chapter 6 concludes the whole system, and represents the future work.

Chapter 2

Background and literature Review

In this chapter we will cover the background material required in the rest of the thesis. We will present an overview of Cognitive Radio Networks, as well as the Physical Layer of LTE/ LTE-A. The last section is the Literature Review of the related works.

2.1 Cognitive Radio

Cognitive Radio Network concept generally talks about sharing a spectrum between two different users. The **primary users** and the **secondary users**. definition of each is presented below:

- Primary User: The primary user is the main user of the specific frequency band. The frequency band is officially licensed to this user.
- Secondary User: The secondary user uses the spectrum when it is not in use by the primary user. It also known as unlicensed user, and has lower priority in utilization of the bandwidth.

When the concept of sharing is brought to discussion, some agreements need to be made, such as:

- The licensed users have the right to take the decision whether to allow cognitive access into their own bands or not.

- The secondary user operates independently from the primary user, but it needs to follow some restrictions, such as the maximum amount of interference that could be imposed on the primary user.

At the time of writing this thesis, there are three main techniques for identifying the so called frequency holes [12]:

- Geographical database: Refers to the list of available spectrum bands for SUs at each geographical points.

- Beacon based sharing approaches: Refers to the transmission of a known signal by PUs as the beacon to inform the SUs that the frequency band will be used by PU.

- Spectrum Sensing: Refers to the action of searching for spectrum holes within the primary signal, which is done by the cognitive device, i.e. the secondary user.

In this work, we use the third technique i.e., *Spectrum Sensing*. The term cognitive radio (CR) was first defined by Joseph Mitola III [13]. According to Mitola, CR technology is the "intersection of personal wireless technology and computational intelligence", where CR is defined as "a really smart radio that would be self-aware, RF-aware, user-aware, and ..." [13].

The rapid evolution in microelectronics has enabled the development of Software-Defined-Radio (SDR) technology, where radio transceivers perform the entire base-band in software. Consequently, any waveform designed in the memory of the SDR platform can be employed on any frequency [5]. Since the cellular standards are based on software, they can be changed "**on the fly**" to adapt to different user needs of

each cell, rather than replacing the radio frequency (RF) hardware, which can be a prohibitively expensive upgrade. Furthermore, new standards can be uploaded to the SDR platform for instantaneous deployment in a cellular region [14]. Cognitive radio hand in hand with SDR can provide functionality considered impossible in the past.

Definitions of Cognitive Radio Networks

The term Software-Defined-Radio (SDR) refers to the implementation of base-band processing in a software based platform. In fact, SDR enables the base-band processing of a digital communication system to be programmable. That is, the operation characteristics of the system can be changed at will, simply by loading a new design. Although, the radios on SDR would be able to change functions and operations, they can do this reconfiguration only on demand. They are not capable of self-reconfiguration to the most effective form without external command or demand. In Mitola's dissertation [13] and a number of publications, he visualized such a self-reconfigurable radio and dubbed the term ***cognitive radio*** for it. According to Mitola's early definition, a CR would be realized through the integration of model-based reasoning with software radio and would be trainable in a broad sense, instead of just being programmable.

Haykin defines CR as a radio capable of being aware of its surroundings, learning, and adaptively changing its operating parameters in real time with the objective of providing reliable anytime, anywhere, and spectrally efficient communication [15].

The U.S. Federal Communications Commission (FCC) uses a narrower definition for this concept: "A Cognitive Radio (CR) is a radio that can change its transmitter parameters based on interaction with the environment in which it operates. The majority of cognitive radios will probably be SDR (Software Defined Radio) but neither having software nor being field programmable is requirements of a cognitive radio".

Despite the differences in the given descriptions of the Cognitive Radio concept,

two main characteristics can be mentioned. First, CRs are re-configurable, and second, they behave intelligently and adaptively. The second term points to the ability of adaptation, without being *a priory* programmed. As discussed above, Cognitive Radio functionality requires at least the following capabilities:

- **Flexibility and agility:** In Cognitive Radio Network, the secondary users should be able to change the waveform and other radio operational parameters in order to not to impose any disturbance on the licensed users.

- **Sensing and Adaptability:** The ability to observe and measure the state of the environment, including spectral occupancy. Sensing is necessary if the device is to change its operation parameters based on its current knowledge of the RF environment ([12], page 7). In Chapters 3 and 4 of the thesis we propose a combined algorithm for sensing the cognitive radio environment.

The work by Mitola and Maguire in 1999, and also the early spectrum measurement studies to quantify the spectrum use both in the licensed and unlicensed bands, conducted as early as in 1995, were the main precursors of CR studies. In the United States, CR research focused quickly on Dynamic Spectrum Access (DSA) and secondary use of spectrum as the main objectives of the initial research. The foundation of our work is to design Cognitive Sensing Algorithm for sensing the LTE/ LTE-A technology as the primary (Licensed) user of a cognitive radio scenario. The design is based on Dynamic Spectrum Sensing, and the algorithm is a real-time sensor.

2.1.1 Cognitive Sensing

Different measurement campaigns reveal that much of the licensed spectrum remains unused, both in time and in frequency [5]. Efficient utilization of the spectrum requires the ability of exploiting instantaneous opportunities at a preferred time scale [16]. To have efficient operating cognitive radio, secondary users should be able to dynamically

exploit the frequency bands, which may be underutilized even for a short period of time. A vital component of cognitive networking is thus spectrum sensing, i.e. to be capable of sensing those available resources. The secondary user (SU) should sense the spectrum precisely, quickly seize opportunities to transmit, and vacate the spectrum once a primary user (PU) reoccupies it. As noted in [17], a critical component of opportunistic spectrum allocation is the design of the spectrum sensor for opportunity detection.

2.1.2 Spectrum Access and Sharing

Spectrum sharing is the simultaneous use of a specific radio frequency band in a specific geographical area by a number of independent entities. The mechanism is different from traditional multiple-access and random-access techniques. The summarized classification of the spectrum access and sharing is depicted in Figure (2.1). Sharing of the licensed spectrum is done either by coordination between the primary and secondary users, or giving lower priority in access to the secondary user, called Secondary Access.

In **Coordination** mode, usually both users have access to the scheduling information. Based on this, they use a scheme to share the spectrum.

On the other hand, **Secondary Spectrum Access** mode, also called SSA, allows the spectrum analysis in real-time and non-real-time paradigms.

The *non-real-time* SSA refers to a situation, where the license owner of a specific band is willing to let a secondary user to access a frequency band for a specific time period and specific location.

On the contrary, the *real-time* SSA refers to the situation where there is no possibility of interaction between primary and secondary users. Under this condition, the secondary system should opportunistically identify and utilize the unused portions of frequency band. The real-time spectrum access sharing could arise two different

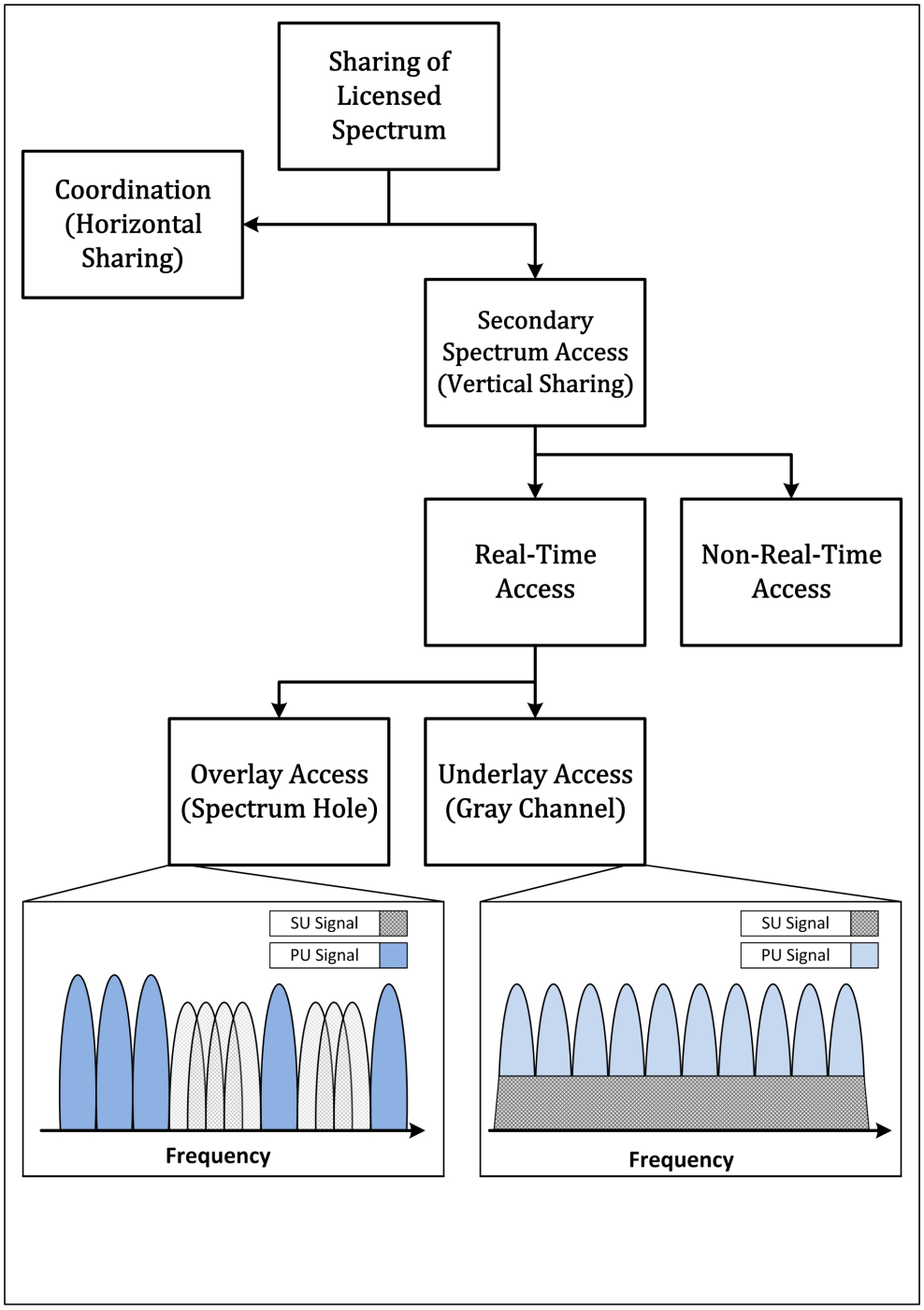

Figure 2.1: Classification of Spectrum Sharing Techniques.

forms of spectrum access: The *Underlay Access*, and the *Overlay Access*.

The underlay access, also known as gray channel access, is the transmission of the secondary system in the portion of frequency band that is actively in use by primary user. This, of course, must be done in a way that there would be no imposing of interference to the primary user. The deterministic solution is ultra-wideband (UWB) transmission schemes ([12], Section 5.6.5).

In overlay spectrum access, (which is the scheme of this work) the Cognitive Radio Device should ideally sense the overall licensed band, in order to identify spectrum holes. It is more probable for the CR to find several small idle bands which are located randomly, rather than a large portion of idle bandwidth.

This work is designed under the Secondary-Spectrum-Access approach to solve the issue of underutilized spectrum. The real-time spectrum hole detection algorithm is proposed in Chapter 4. The access technique for reusing the detected frequency bands is overlay, meaning that the secondary user transmits on unused portions of frequency band for a priori known time duration. For more reading on the spectrum sharing techniques we refer the interested reader to Chapter 5 of [12].

2.2 LTE-Downlink Schematic

Long Term Evolution or LTE standard was developed to support high data rate and a large number of users. LTE is the next evolutionary step after the 3G, and the standardization is developed by Third Generation Partnership Project (3GPP). Many of technological features have not been implemented, but due to its unique and well specified design it is known as the first global wireless standard. LTE bring together many technologies and innovation. One can say LTE will change the way we use mobile networks in near future. The detailed specification and standardization of LTE technology is easily accessible, e.g. [1]. So, we only cover the aspects that

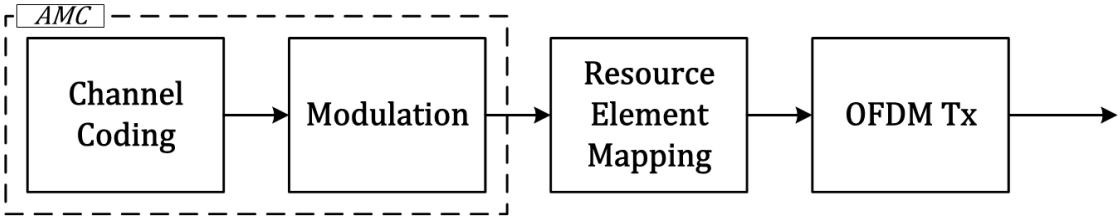

Figure 2.2: Overview of DL Transport Channel

are needed for better understanding of the work. In our Cognitive Sensing scheme, we achieve timing information of the primary user (LTE system). The algorithm also checks the time-frequency grid for empty blocks. Therefore, we present both time and frequency structure of the LTE-Downlink signal, as well as time synchronization procedure in LTE-Downlink. In summary, we briefly cover the LTE-DL physical layer block diagram, frame structure, random access, and synchronization procedure.

2.2.1 LTE Down-Link Physical Layer

A brief overview of LTE-Downlink physical layer, which is useful for following the developed sensing algorithm, is presented.

Adaptive Modulation and Coding Scheme

LTE systems employ adaptive modulation and coding (AMC) in order to take advantage of fluctuations in the channel over time and frequency. The basic idea is quite simple. Transmit at high data rate as much as possible when and where the channel is good, and transmit at a lower rate when and where the channel is poor in order to prevent excessive dropped packets. By lowering data rate we mean lowering the order of modulation scheme to let say QPSK and low rate error correction coding such as rate $\frac{1}{3}$ turbo code. Different coding rate and different modulation scheme are chosen for transmission according to the feedback provided from the channel known as Channel Quality Indicator (CQI). Based on them the code rate and also modulation

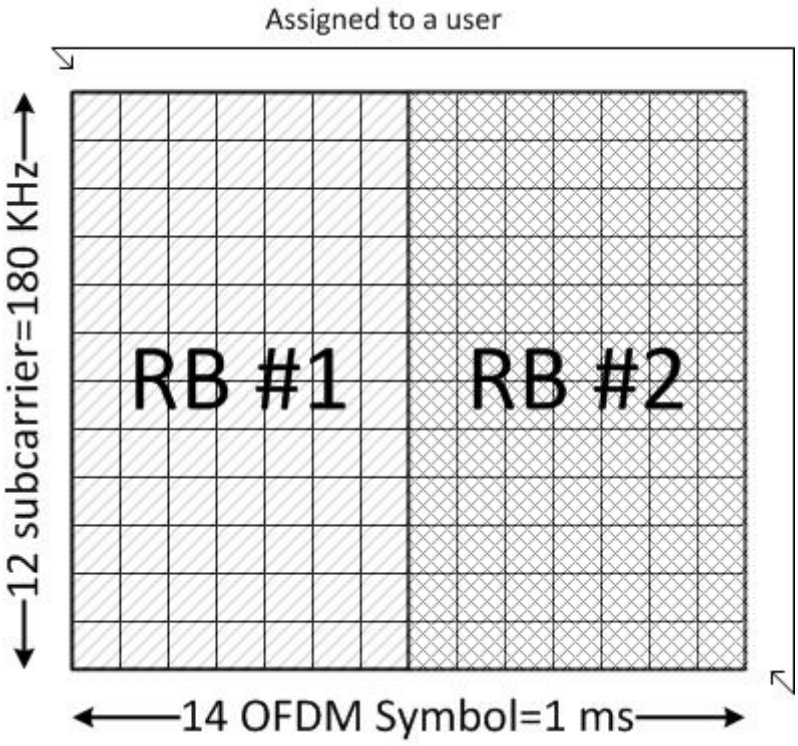

Figure 2.3: LTE DL Resource Block Grid Illustration.

order are chosen for Downlink transmission.

Resource Element Mapping

In LTE resource Grid illustration, the smallest unit consists of the frequency band equal to sub-carrier spacing, and the duration of one OFDM symbol, is called resource element. Each of these resource elements (RE) could carry one modulation symbol, which in Down-Link could be a Q-PSK, 16-QAM or 64-QAM symbol. The grid of 12 frequency sub-carriers index and 7 time OFDM symbols [1] make a Resource Block (RB) as it is shown in Figure (2.3). Each two adjacent RBs in time, make the smallest scheduling assignment, which is called Resource Block Pair (RBP).

[1]Normal Cyclic-Prefix Mode, frame structure type 1. For more information see [1]

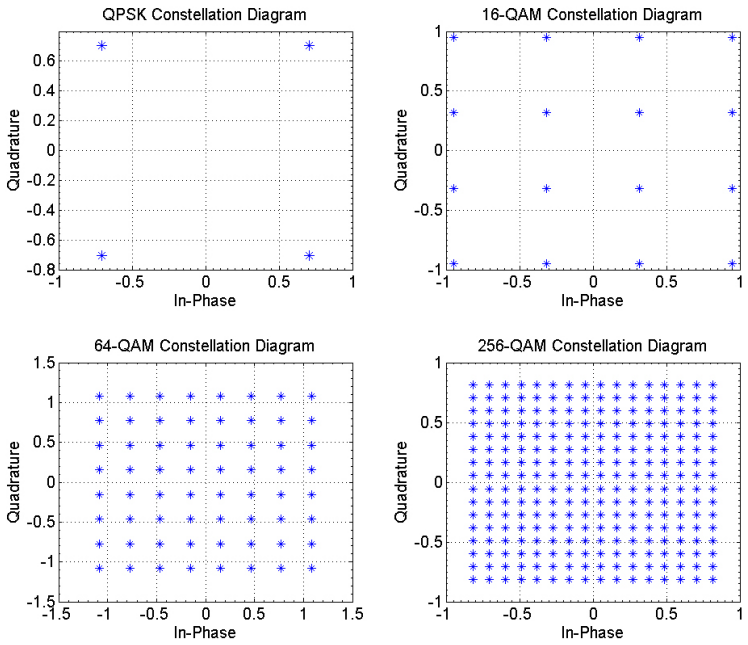

Figure 2.4: QPSK, 16-QAM and 64 QAM constellation diagram based on [1], and also 256-QAM

Downlink OFDM Transmission

OFDM stands for Orthogonal-Frequency-Division-Multiplexing, and uses the orthogonality between sub-carriers in frequency domain to overcome the Inter-Symbol-Interference (ISI). It is a multi-carrier transmission scheme which breaks a high rate stream of data symbols into low rate parallel streams. Each of these streams transmitted on a carrier, which is called sub-carrier. The sub-carriers are designed to be orthogonal to each other in frequency. OFDM transmitter/receiver could be implemented in two ways.

1. Using orthogonal modulators and filter bank.

2. IFFT/FFT based implementation of OFDM.

Due to low complexity of FFT(IFFT), particularly, when the size is a power of two, LTE and other standards like IEEE 802.11 (WiFi) use IFFT/FFT based implemen-

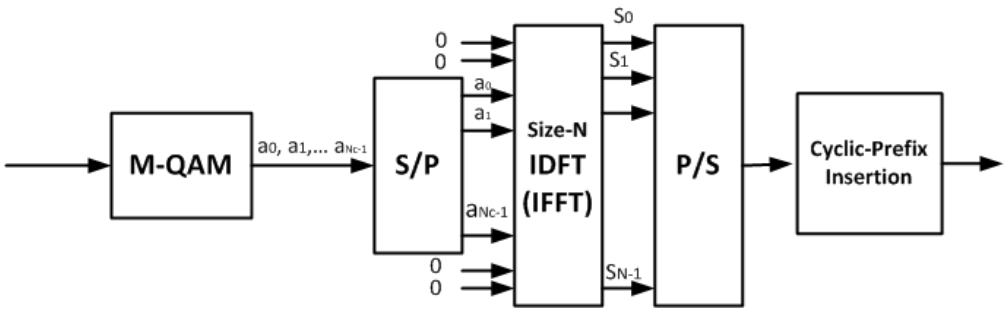

Figure 2.5: LTE-DL OFDM Transmission Block Diagram

tation. Let's define a_k as M-QAM modulation symbol ($\{k = 0, \ldots, N_c - 1\}$), that is chosen from one of the constellation diagrams presented in Figure (2.4), according to Adaptive Modulation and Coding scheme decision. N_c is the total number of sub-carriers. These symbols are the inputs of OFDM block. As it is shown in Figure (2.5), the OFDM block basically consists of serial to parallel, IFFT, parallel to serial, and Cyclic-Prefix Insertion processes. The presented block is formulated as:

$$s_n = s(nT_s) = \sum_{k=0}^{N_c-1} a_k e^{j2\pi k\Delta f n T_s} = \sum_{k=0}^{N_c-1} a_k e^{j2\pi kn/N} \tag{2.1}$$

where N is the IFFT size, and Δf is the sub-carrier spacing. k is the sub-carrier index, and n is the sample number. This is the IDFT process which can be implemented using IFFT.

Note 1: Unlike a_k, s_n does not have a specific constellation diagram. They could be located anywhere in the I-Q diagram.

Note 2: Cyclic-Prefix insertion is performed by adding a copy of a certain number of samples from the end of OFDM symbol to its beginning (Figure 2.6).

One reason for CP insertion, is to surpass the effect of Doppler Spread, caused by mobility of the users. CP insertion will guarantee the sub-carriers to remain orthogonal for up to a specified speed of mobility.

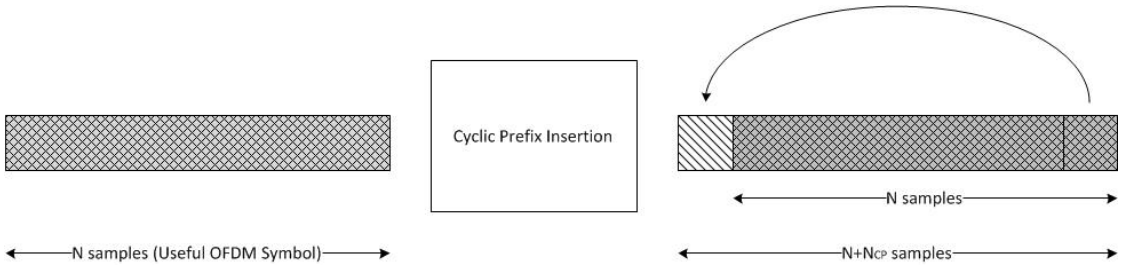

Figure 2.6: Cyclic-Prefix Insertion

2.2.2 LTE Down-Link Signal Structure

LTE-DL signal is illustrated as a time-frequency grid in [1]. For clarification on raw signal time and frequency characteristics, we first present the timing structure.

Time Domain Frame Structure

LTE is designed to operate in both FDD and TDD mode of operation. Also two types of frame structure are considered for Downlink in the standard. In this work, we study the FDD mode of operation and frame type one. So the following is LTE Downlink frame structure type 1, operating in FDD mode. For other operational mode and frame structures, see LTE standardization.

LTE design specification defines a frame as 10 ms length signal, consisting of 10 sub-frames of 1 ms each. The scheduling updates are applied for each sub-frame.

Now consider each sub-frame as two time slots. In normal CP mode each slot consists of 7 OFDM Symbols, in which the first has the duration of 71.76 μs, and the others have 71.36 μs. This difference in duration of OFDM symbols is due to different Cyclic-Prefix length, and is shown in Figure (2.7).

$$T_{OFDM-Symb} = T_u + T_{CP} \tag{2.2}$$

To provide consistent and exact timing definition, different time intervals within the LTE specification are defined as a multiple of a basic time unit, $T_s = 1/(15000.2048)$

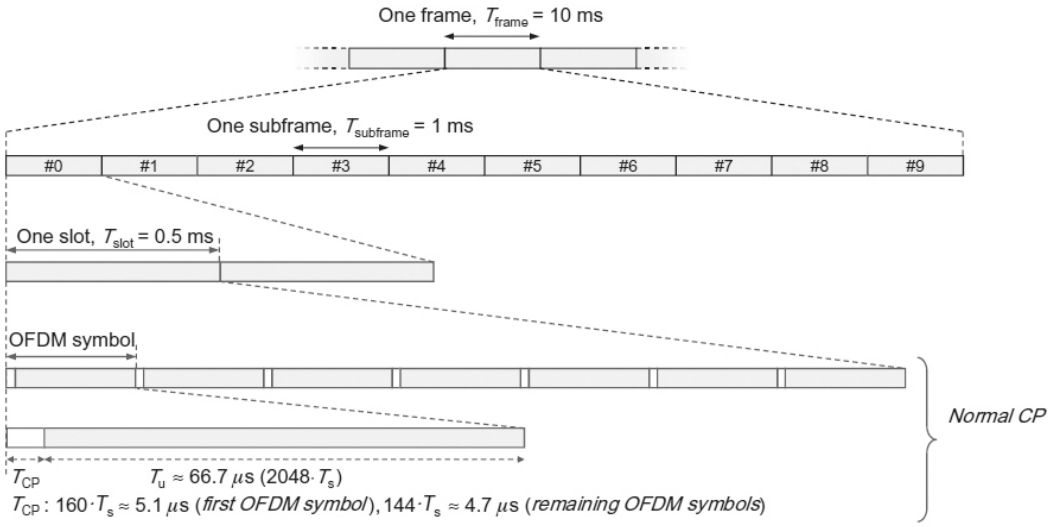

Figure 2.7: LTE DL Frame Structure

seconds. This basic time can be seen as sampling time of an FFT-based Transmitter/Receiver implementation with the FFT size of 2048. Figure (2.7) shows the LTE frame structure. The frame duration time is T_{Frame}, and equal to $307200.T_s$. The Cyclic-Prefix length for first OFDM symbol of a slot, T_{CP}, is equal to $160.T_s \approx 5.1\mu s$, and for other OFDM symbols of a slot is equal to $144.T_s \approx 4.7\mu s$. Then the useful OFDM symbol duration is $T_u = 2048.T_s \approx 66.7\mu s$.

Frequency Domain Signal Structure

LTE can operate in minimum bandwidth of 1.4 MHz (bandwidth of 6 RBs) to 20 MHz (100 RBs). Also up to 5 of these bandwidths (each called Component Carrier (CC)) could be aggregated to shape up to 100 MHz of transmission bandwidth (LTE Advanced). Component Carriers are configured independently, and each contain different number of RBs. The bandwidth of a resource block consists of 12 sub-carrier each with 15 KHz bandwidth (FDD mode). The minimum bandwidth that could be assigned to a user is the bandwidth of a Resource Block (RB), which is 180 KHz. So we can define an RB as a time-frequency block of 12 sub-carriers for the duration of

one time slot (0.5 ms). That means a sub-frame duration consists of 2 RBs duration. A pair of adjacent RBs is the minimum resource that can be assigned to a user. Figure (2.3) shows a pair of RBs, which are assigned to a user.

2.2.3 LTE-DL Synchronization Process

The following procedures need to be done by an LTE terminal before being able to communicate with the network.

- Cell Search: Find and acquire synchronization to a cell (base station: eNode-B) within the network.
- Cell System Information Reception: Receive and Decode the information, also known as the cell system information, required for proper communication within the cell, such as frequency-time location of reference symbols and pilots.

Once these two processes have been completed, the terminal can access the cell by means of random-access procedure (see [10]).

Overview of Cell Search

To remain synchronized, and support mobility, an LTE terminal in not only required to carry out the cell search at the power up (initially accessing the system), but also it requires to continuously perform similar procedure. This will also provide the chance of evaluating the reception quality of the neighboring cells, to conclude if the handover or cell re-selection should be carried out. The main parts of the cell search procedure are:

- Acquisition of frequency and symbol (time) synchronization to a cell.
- Acquisition of frame timing of the cell, that is, to determine the start of the Downlink frame.

- Determination of the physical-layer cell identity of the cell [10].

From the above, we only present the first two parts, as they will be required for understanding of the thesis. For a complete discussion on this subject, we refer the reader to Chapter 4 of [10].

On each Downlink component, two special signals are transmitted for assisting the cell search and synchronization procedure. The ***Primary Synchronization Signal*** known as PSS, is transmitted within the last OFDM symbol of the first slot of sub-frames 0 and 5. While the ***Secondary Synchronization Signal***, known as SSS, is transmitted within the second last OFDM symbol of the same slot (one OFDM Symbol prior to PSS). The PSS signal is transmitted twice within LTE-DL frame, and it could take three different values to show the **Cell Number** in physical-layer cell identity procedure. Once the terminal has detected and identifies the PSS of the cell, it has found the following:

- Five-millisecond timing of the cell and thus also position of the SSS, which has a fixed offset relative to the PSS.

- The Cell Number within the cell-identity group, which can be one of 3 values of 0, 1, and 2.

Up until here, the terminal has not found the exact frame timing of the system, however, it has acquired the start of the OFDM Symbols within a sub-frame, which is enough for the proposed sensing algorithm in Chapter 4. So basically, what we propose in Chapter 3, is the blind detection of the PSS in order to find the beginning of each sub-frame, not the Frame.

The LTE terminal requires to detect the frame timing as well. So by detecting the position of the SSS, which is known once the PSS has been detected terminal will find the following:

- Frame timing

- Cell Group Number (which can be one value from 0 to 167).

In short, by detecting the PSS and SSS, an LTE terminal not only achieves the Downlink frame timing of the system, but also determines the Cell ID of the cell by the formula below:

$$Cell\ \ ID = 3 \times Cell\ Group\ Number + Cell\ Number \tag{2.3}$$

As the sub-frame timing is only required for this work, we only present the primary synchronization signal structure.

PSS Structure

The three PSS alternatives are three length-63 Zadoff-Chu (ZC) sequences extended with five zeros at each edge and mapped to the center 73 sub-carriers (six center RBs) as illustrated in Figure (2.8). It should be noted that due to coinciding with DC sub-carrier, the central sub-carrier will actually not be transmitted. (element X_{32}^{PSS} is not transmitted). The PSS thus occupies 72 resource elements (not including the DC carrier) in sub-frame 0 and 5 while operating in FDD mode. In [1] (section 6.11.1), the sequence $d(n)$ used for PSS is generated from the frequency-domain ZC sequence and defined as:

$$d_u(n) = \begin{cases} e^{-j\frac{\pi un(n+1)}{63}} & n = 0, 1, \ldots, 30 \\ e^{-j\frac{\pi u(n+1)(n+2)}{63}} & n = 31, 32, \ldots, 61 \end{cases} \tag{2.4}$$

where u is the root for ZC sequence and can take values 25, 29, and 34, corresponding to Cell Numbers 0, 1, 2 respectively. As it is mentioned, detecting this signal is equal to finding sub-frame timing of LTE signal.

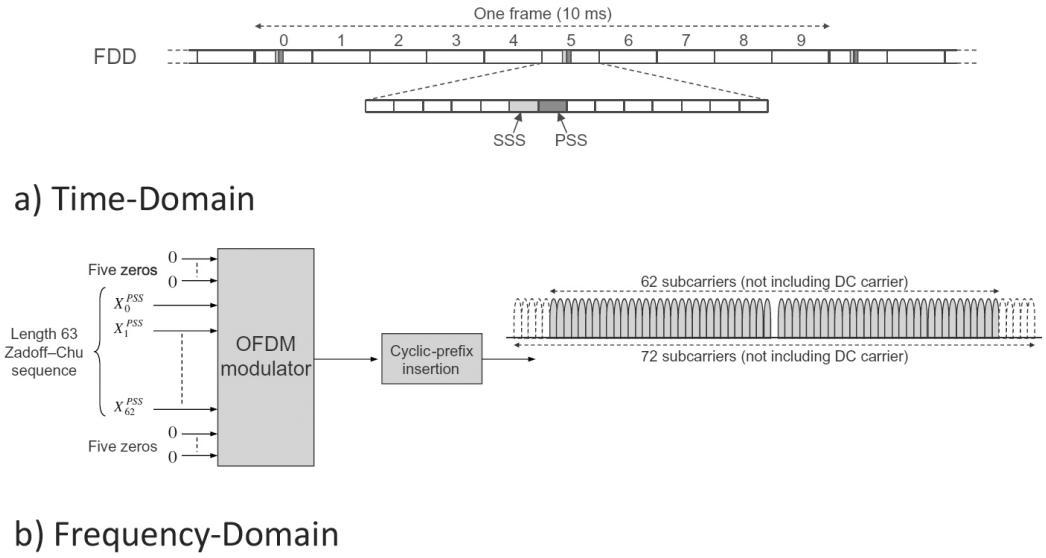

Figure 2.8: PSS Structure

2.3 Literature Review

In this section, we review some literature on 1) cyclostationarity properties of the wireless signals, 2) Algorithm for fast and accurate detection of PSS, 3) concepts related to cognitive sensing and the interference produced to the primary user of cognitive radio network.

2.3.1 Cyclostationarity property of OFDM Signals

In [18], Ning Han and others used the cyclostationarity properties of OFDM signal to first recognize it from the Gaussian noise, and also identify its transmission characteristics such as the sub-carrier spacing, guard interval, and OFDM symbol Duration. They proposed a simple but reliable peak detection method for detecting the OFDM signal, and a peak searching method for identification step. All the process have been done without any prior knowledge of the signal, that is why they call the algorithm blind detection.

In [19] Al-Habashna and others propose an algorithm which uses not only the cyclic-prefix cyclostationarity but also the preamble, and reference symbols of both mobile WiMAX and LTE signals. In this paper, authors show that the algorithm is immune to phase, frequency, and timing offsets.

2.3.2 Algorithms for PSS Detection

In [20] Wen Xu, K. Manolakis, proposed a multi-step method for accurate time and frequency synchronization in LTE system. They first grossly achieve the symbols within LTE signal using cyclic-prefix detection, and then based on cross correlation they could locate the beginning of frame or beginning of the half frame.

In [21] and [22], Zhongshan Zhang, Ming Lei and others study the improved PSS detection algorithm by exploiting the central-symmetric structure of the ZC sequences. They first propose a low-complexity detector with almost half the complexity of non-coherent conventional detector, and the same accuracy. They also proposed an improvement based on the central-self-correlation property of PSS, to reduce the complexity to even half of the latter. They have evaluated the performance of all their proposed algorithms in terms of the PSS acquisition time.

2.3.3 Cognitive Radio Networks and Similar Works

In [23] Mai Vu, Saeed S. Ghassemzadeh, and Vahid Tarokh consider a cognitive network, where the cognitive users are uniformly distributed around single primary user. They consider a scheme in which the primary user transmitter sends beacon signaling on its own transmission. As soon as the cognitive user detects that beacon, it should vacate the frequency channel, otherwise interference is produced. The mean and variance of the interference is calculated as well as their relation to the outage probability on the primary user.

In [24], F. Shayegh and M. Reza Soleymani considered an OFDM-based cognitive

network where a secondary user chooses parallel sub-channels from different primary users' bands to form its transmission link. Like [23] the primary users transmits beacon in prior to their transmission, and by detecting that beacon, secondary users should leave the band. The total mean and variance of the interference is calculated. An analytical lower bound on the mean of the capacity is provided, and the trade-off between the capacity and the interference is evaluated.

Chapter 3

Obtaining the Subframe Timing of LTE Signal

In this chapter, we present an algorithm for obtaining LTE sub-frame timing, without having any previous knowledge of LTE signal. This algorithm acts like a startup procedure at the beginning of **Cognitive Sensing** algorithm. The timing information will be used in both Spectrum Hole Detection (SHD) process and secondary user transmission scheme, so the accuracy of timing information is very important. The algorithm is designed based on sequence detection within the received signal. Although it has always been a trade off between the observation time and the performance of a detection algorithm and some studies consider that to evaluate the performance, we did not do so. Instead, we analyze the performance with respect to the received signal to noise ratio (SNR). At first stage, we use Cyclic Auto-correlation Function (CAF) to detect the cyclostationarity property of LTE Downlink signal to obtain the OFDM symbol boundaries. This will considerably reduce the processing load in the second stage which is Primary Synchronization Signal (PSS) detection. The PSS is transmitted by the primary user every five-milliseconds. Thus, once the PSS is detected, the sub-frame timing is obtained. To reduce the possibility of wrong

timing information, we apply the Constant False Alarm Rate (CFAR) algorithm to the PSS detection stage. This algorithm removes the dependence of false alarm probability (the probability of catching wrong timing information) to SNR. The proposed scheme for detecting the PSS has a previous step, which makes it different from one used in original process in LTE. That is the using of the cyclostationarity properties for finding the boundaries of the received signal that may contain the PSS, or not. This basically reduce the processing load of the process.

3.1 OFDM Subframe Boundary Detection

The Cyclic Auto-correlation Function (CAF) gives the symbol boundaries of LTE-Downlink signal by detecting the cyclostationarity properties of OFDM signal. This will be used in the PSS detection step for reducing the processing load. When the boundaries of the symbol that may carry the PSS are known, one may separately check each *OFDM symbol* of the received signal. Otherwise, without having OFDM symbol boundaries, for detecting the PSS using conventional cross-correlation and simple peak detection, the detector should continuously check the received signal *sample by sample* until the correlation shows the peak.

3.1.1 Cyclostationarity property of OFDM signal

In the OFDM transmission scheme, the cyclic prefix (CP) insertion is done for every OFDM symbol. The CP insertion guarantees the orthogonality between the subcarriers. However, from stochastic point of view, the CP insertion causes the periodic behavior of the statistical properties of the signal. In other words, the mean and auto-correlation function of the OFDM signal exhibit the periodicity properties, which said to be *cyclostationarity* in wide sense.

Considering uncertainty in the detector, we use a two-step detection approach for

blind detection and identification of the OFDM signal from random noise. In this section, by the term detection we mean recognizing the OFDM signal from noise. Also by identification, we mean finding the OFDM parameters such as sub-carrier spacing and duration of guard intervals. The main advantage of using cyclostationarity properties of OFDM signal is that the detector does not need to perform FFT process, since the number of sub-carriers is unknown, the mismatch of FFT parameters will reduce the performance of any FFT based detection method [18]. The first step is to detect the OFDM signal from random noise. This could be done by recognition of symmetric peaks in auto-correlation function of the received signal. This function is a special case of the cyclic auto-correlation function (CAF). This step also provides the sub-carrier spacing of OFDM signal if it exists. The second step is to identify the OFDM signal using sub-carrier spacing, found in previous step. Considering the CAF function for a specific time shift equal to the inverse of sub-carrier spacing, the distance between peaks estimate the inverse of the OFDM symbol duration.

A. Definition of CAF

A process for instance $x(t)$, is said to be cyclostationarity in the wide sense if its mean and auto-correlation are both periodic with some period, say T [25]:

$$E[x(t+T)] = E[x(t)] \tag{3.1}$$

$$R_x\Big(t+T+\frac{\tau}{2}, t+T-\frac{\tau}{2}\Big) = R_x\Big(t+\frac{\tau}{2}, t-\frac{\tau}{2}\Big) \tag{3.2}$$

where $R_x(t+\frac{\tau}{2}, t-\frac{\tau}{2})$, the auto-correlation function of two independent variable t and τ, is periodic in t with period T for each value of τ. Then the associated Fourier series for this function is:

$$R_x\Big(t+\frac{\tau}{2}, t-\frac{\tau}{2}\Big) = \sum_{\alpha} R_x^{\alpha}(\tau).e^{i2\pi\alpha t} \tag{3.3}$$

for which

$$R_x^{\alpha}(\tau) = \frac{1}{T} \int_{-T/2}^{T/2} R_x(t,\tau) e^{-i2\pi\alpha t} dt \tag{3.4}$$

are the Fourrier coefficients. Sum over α includes all integer multiples of the reciprocal of the fundamental period T. Letting the α range over all integer multiples of all fundamental frequencies of interest, the model for R_x shows more than one periodicity. But the equation 3.4 must be modified.

$$R_x^{\alpha}(\tau) = \lim_{T\to\infty} \frac{1}{T} \int_{-T/2}^{T/2} R_x(t,\tau) e^{-i2\pi\alpha t} dt \tag{3.5}$$

Then the associated $R_x(t,\tau)$ is said to be an almost periodic function of t [26]. Then the signal is showing cyclostationarity property if there exists a periodicity frequency α for which the R_x^{α} in equation 3.5 is not identically zero. The function $R_x^{\alpha}(\tau)$, which is the amplitude of the sinusoid in t at frequency α in the R_x function, is referred to as the *cyclic auto-correlation function* (CAF). The set $\{\alpha \ : \ R_x^{\alpha}(\tau) \neq 0\}$ is referred to as the set of *cyclic frequencies*.

B. CAF of Base-band OFDM Signal

The CAF of base-band OFDM signal can be calculated as [27]:

$$R'^{\alpha_n}_x(\tau) = \frac{A}{T_{symb}} . \frac{sin(\pi n \Delta f \tau)}{sin(\pi \Delta f \tau)} . e^{j2\pi\Delta f \frac{n-1}{2}\tau} \times \int_{-\infty}^{\infty} G(f) G(\alpha_n - f) df \tag{3.6}$$

where $G(f)$ is the Fourier transform of the rectangular pulse shape $g(t)$. A is the variance of the symbol sequence. $T_{symb} = T_u + T_{CP}$ is the OFDM symbol duration, where $T_u = 1/\Delta f$ is the useful OFDM symbol duration, $T_{CP} = T_g$ is the duration of guard interval and Δf is the sub-carrier spacing. In this study the $\frac{A}{T_{symb}}$ has got constant value, and also we are interested in detecting the peak values. So we

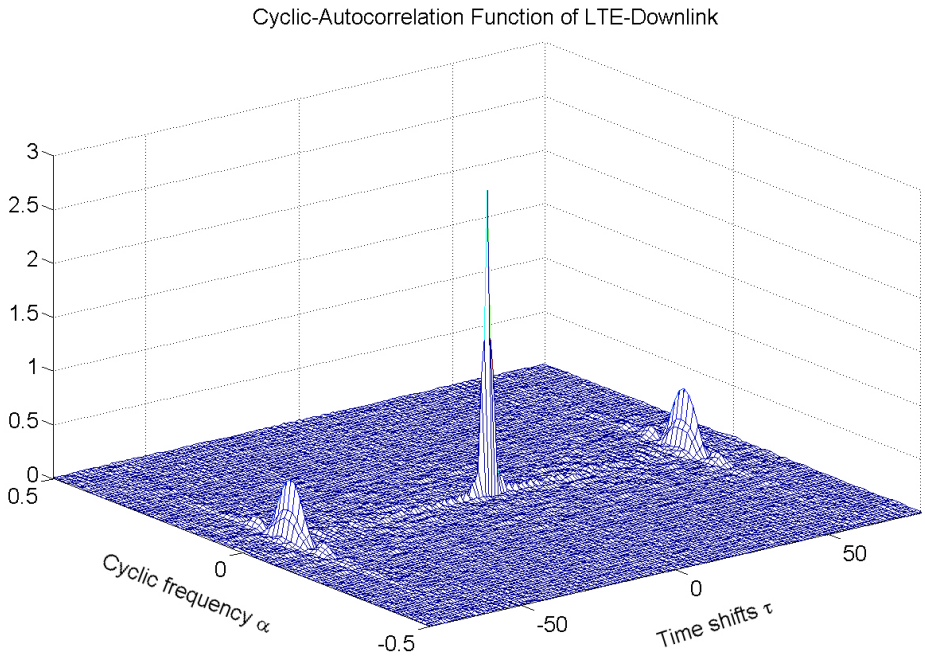

Figure 3.1: CAF of LTE-Downlink for an OFDM Symbol

normalize the formula to that:

$$R_x^{\alpha_n}(\tau) = \frac{sin(\pi n \Delta f \tau)}{sin(\pi \Delta f \tau)} . e^{j2\pi\Delta f \frac{n-1}{2}\tau} \times \int_{-\infty}^{\infty} G(f)G(\alpha_n - f)df \tag{3.7}$$

The signal exhibits discrete cyclic auto-correlation surfaces for the cyclic frequencies $\alpha_n = n/T_{symb}$, which peak at $\tau = \pm\frac{1}{\Delta f} = \pm T_u$ where the factor $sin(\pi n \Delta f \tau)/sin(\pi \Delta f \tau)$ takes its maximum value. As it is shown in Figure (3.1), by knowing the values of T_{symb} and T_u, the peaks are easily detectable. However, in blind detection and identification, the parameters of the received signal are unknown. It means that the values of α at which CAF exhibit peaks are not clear a priori.

C. OFDM signal detection based on Auto-correlation Function

For blind detection of OFDM signal consider two hypotheses test:

$$\begin{cases} H_0: & y(t) = w(t), & signal \quad absent \\ H_1: & y(t) = s(t) + w(t), & signal \quad present \end{cases}$$

where $y(t)$ is the received signal, $s(t)$ and $w(t)$ represent the OFDM signal and noise respectively. As described previously, the peaks in the CAF of OFDM signal are mainly due to the cyclic prefix in OFDM symbol. This feature is employed as the main criterion for separating OFDM signal from noise.

By setting $\alpha = 0$, the CAF will be reduced to Auto-correlation function. So based on the characteristics of OFDM signal with cyclic prefix, the symmetric peaks will happen with time period equal to useful OFDM symbol duration at the output of auto-correlation function. For the peak to be detected, the formulation below shows the statistic test [18].

$$Z_{det} = |R_s^0|^2 = \left| \frac{sin(\pi N \Delta f \tau)}{sin(\pi \Delta f \tau)} . e^{i2\pi \Delta f \frac{N-1}{2} \tau} \times \int_{-\infty}^{\infty} G(f)G(-f)df \right|^2 \tag{3.8}$$

$$= \left| \delta(\tau) \left(\frac{sin(\pi N \Delta f \tau)}{sin(\pi \Delta f \tau)} \right) \right|^2$$

From this analysis, Z_{det} takes the largest peak when $\tau = 0$, and two other peaks when $\tau = \pm T_u$, which is our expectation. By simply finding the number samples between the two symmetric peaks, we found T_u. Since sub-carrier spacing ($\Delta f = 1/T_u$) is determined, it could be used for identification step. The Figure 3.2, shows the Auto-correlation function of LTE-Downlink with received $SNR = 3 \ \ dB$.

D. OFDM identification using Cyclic Auto-correlation Function (CAF)

As explained before, different OFDM signals can be classified by the parameters such as the length of guard interval (cyclic prefix length), sub-carrier spacing. In the

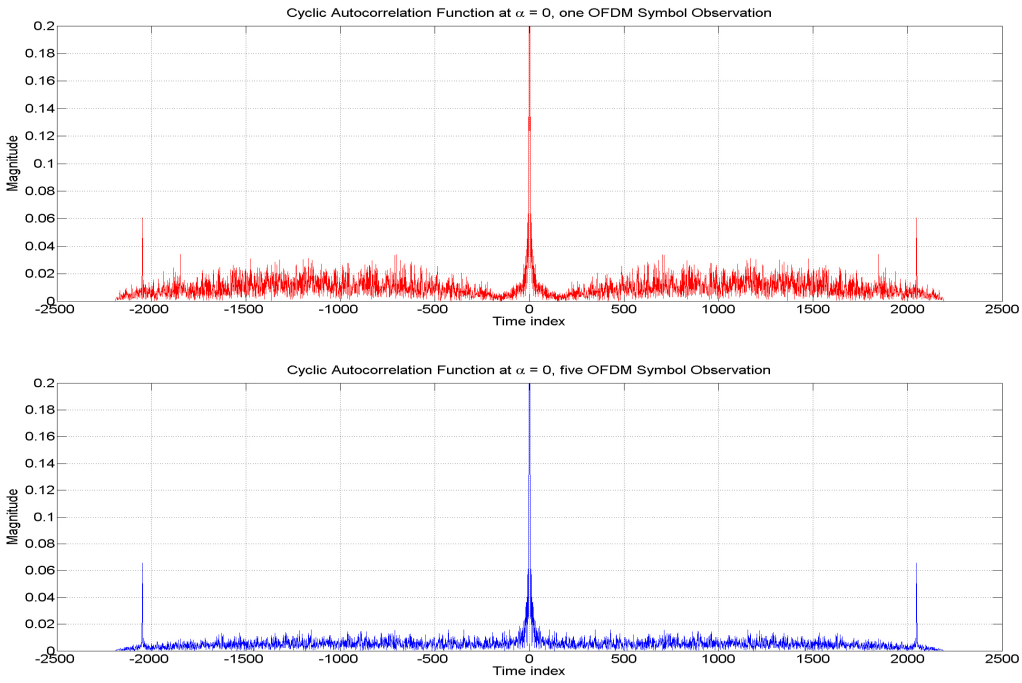

Figure 3.2: The auto-correlation of LTE-Dwonlink signal with respect to τ

first step of the presented scheme, sub-carrier spacing is detected while detecting the OFDM signal. In this step, we find the cyclic prefix length T_{CP} of the received signal. Since the duration of useful symbol has been determined in the first step, we can observe the CAF for $\tau = T_u$. By setting the $\tau = T_u$ in (3.7), the test statistic could be expressed as a function of α_n, as described in the following [18]:

$$Z_{id} = |R_s^{\alpha_n}(T_u)|^2 = \left| \frac{sin(\pi N \Delta f T_u)}{sin(\pi \Delta f T_u)} . e^{i2\pi\Delta f \frac{N-1}{2} T_u} \times \int_{-\infty}^{\infty} G(f)G(\alpha_n - f)df \right|^2 \qquad (3.9)$$

Only the integration of the pulse shaping term is determining Z_{id}. To be able to find T_{symb} from the equation, the step size of α_n is important. The step size between samples of α_n should be small enough, in order to have enough details of CAF pattern. Then, we will be able to observe the peaks. In [18], the step size is chosen equal to 1/20 of sub-carrier spacing Δf. Therefore, the distance between two adjacent peaks is equal to the reciprocal of the OFDM symbol duration, T_{symb}. Then the cyclic-prefix

duration T_{CP} could be easily achieved by the following:

$$T_{symb} - T_u = T_{CP} \tag{3.10}$$

The sample rate of cyclic frequency values is achieved in the study at [18]. In conclusion, the cyclostationarity property of OFDM signal is exploited to find the parameters like sub-carrier spacing, symbol duration, symbol boundaries, and useful symbol duration. For further studies on cyclostationarity properties of man-made signals we refer the interested reader to [25], [19] and [28].

3.2 Detecting the LTE Primary Synchronization Signal

In this section we present PSS detection based on cross-correlation for obtaining the sub-frame timing of the primary user. However, performing this function over all samples of the received signal is very energy consuming. So we rely on the previous section of this chapter, to reduce the processing load by knowing region where PSS may be present. But for introducing the algorithm, we first use complete cross-correlation function to detect the PSS within an LTE Signal.

The PSS detection could be performed either in frequency domain, or time domain. In the first scenario, we assume the detector is equipped with FFT function of the primary receivers. Thus the cross-correlation will be performed in frequency domain, between the FFT of the received signal, and the 63-length ZC sequence. This method requires continuously taking the FFT from the received signal.

In the second scheme, instead of taking the FFT of the received signal, we take the IFFT of the 63-symbol sequences and correlate it with the received signal (in time domain). This method is much faster that the first scenario, as the IFFT of the ZC

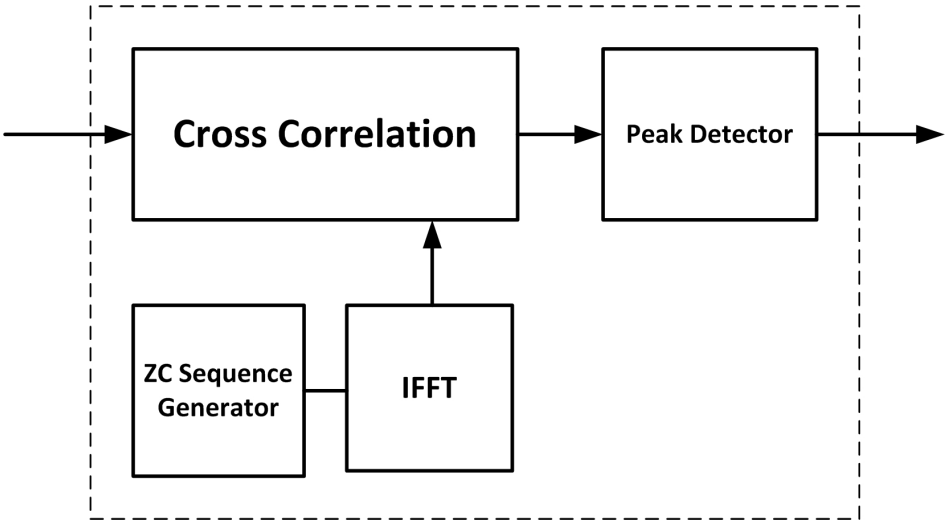

Figure 3.3: block diagram of the PSS detector

sequence could be recorded in a memory. There will be no need for continuously taking the FFT/IFFT of a signal, and also less constraints are applied for implementation. For these reasons, we only consider the second scheme, and we will evaluate it in terms of probability of miss and false alarm.

3.2.1 PSS Detector without OFDM receiver

Consider a detector which is not equipped with FFT processor, and performs the correlation in time domain. For this assumption, the result of the cyclostationarity section is necessary for reducing the energy consumption and processing load. It reduces the number of multiplications required for PSS detection process, from blind detection to a situation that the sensor is aware of the regions where PSS may be present. Consider the PSS detector using the cross-correlation function, one input is the raw samples of the base-band OFDM signal. The other input is the IFFT of length-63 ZC sequence. Figure 3.3 shows the block diagram of the system. One may ask, without knowing the IFFT parameters of the signal, how is it possible to produce proper IFFT version of PSS sequences. The answer is hidden in the

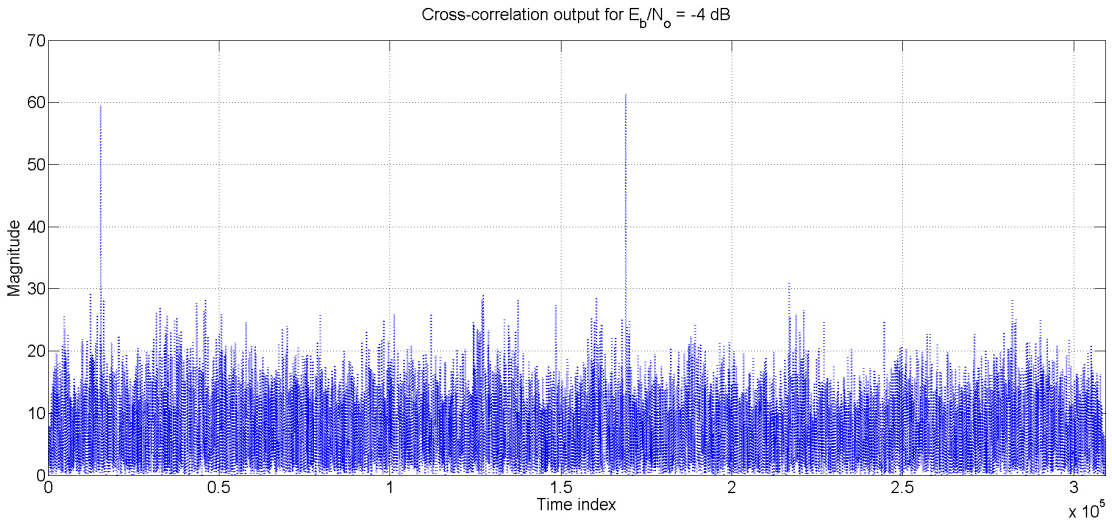

Figure 3.4: Cross-correlation of raw channel signal and IDFT of PSS

LTE standardization. As long as the sub-carrier spacing and the length of cyclic prefix is known (see previous section) the LTE configuration is known and that will give the IFFT size. Then the replica for different sectors with different Downlink configurations could be simply stored in a memory. For more information see Chapter 2 of this thesis, or [1]. Now the cross-correlation function is modeled as:

$$Q_u(n) = \sum_{c=0}^{N_{IFFT}-1} R_u^*(c)y(n+c) \tag{3.11}$$

where $R_u(c)$ denotes the IFFT of u^{th} root of synchronization signal, and $y(n)$ are the samples of the base-band received OFDM signal. The magnitude of the correlation term $|Q_u(n)|$ corresponding to the geographical region with highest signal level shows a significant peak at the time instant when received signal and replica coincide. As the three different replicas are orthogonal the IFFT of them are still uncorrelated, then the other two correlation terms show no peaks. This is shown in Figure 3.4. The algorithm could be performed on every received sample. This means that the detector doesn't have to wait for the whole LTE OFDM Symbol to arrive and then

$N_{ID}^{(2)}$	Root index u
0	25
1	29
2	34

Table 3.1: Root indexes for the PSS

check for PSS location. Our purpose is to detect the presence of PSS, in LTE frame, then we can find the beginning of each sub-frame.

3.3 Probability of Miss Detection and False Alarm

In this section we calculate the probability of miss detection and false alarm for detecting the PSS.

3.3.1 Miss Detection and False Alarm

Consider the 63-length Zadoff-Chu sequence(see Chapter 2) as a PSS sequence.

$$ZC_u^{63}(n) = exp\Big[\frac{-j\pi un(n+1)}{63}\Big] \tag{3.12}$$

where, $n = 0, 1, ..., 62$, and $u \in \{25, 29, 34\}$ stands for the ZC sequence root. For a given u, $ZC_u^{63}(31)$ is not used to avoid modulating the DC sub-carrier, and the remaining elements of the sequence can be represented as:

$$\mathbf{z}_u = [ZC_u^{63}(0), ..., ZC_u^{63}(30), 0, ZC_u^{63}(32), ..., ZC_u^{63}(62)]^T \tag{3.13}$$

ZC sequences with different roots have low cross-correlation among them and enable high PSS identification capability in practice [29].

The z_u is located in the middle of the parallel input of the IFFT block of the OFDM transmitter. We denote by $s^0(n)$ the received OFDM symbol when it does not have a PSS, and $s^1(n)$ when the OFDM symbol contains the PSS. The received

signal $s^1(n)$ is generated at the LTE-Downlink as follows:

$$s^1(n) = s(nT_s) = \sum_{k'=0}^{N-1} a'_k . e^{j2\pi . k . \Delta f . n . T_s} = \sum_{k'=0}^{N-1} a'_k . e^{j2\pi . k' . n/N} \tag{3.14}$$

where $a_{k',l}$ is the input of the IFFT for the l^{th} OFDM symbol which carries the PSS.[1] Now, consider k (not k') as the sub-carrier index from zero to $N_{sc} - 1$, while N_{sc} is the total number of sub-carriers, the length of $a_{k,l}$ is not necessarily a power of two.

$$a_{k,l} = [x_0, ..., x_{N_{sc}/2 - N_{ZC}/2}, \mathbf{z}_u, x_{N_{sc}/2 + N_{ZC}/2}, ..., x_{N_{sc}-1}] \tag{3.15}$$

where x_n are the data symbols. By adding zeros at both side of the $a_{k,l}$, we define $a_{k',l}$ as follows:

$$a_{k',l} = [0, ..., 0, a_{k,l}, 0, ..., 0] \tag{3.16}$$

where k' is from zero to $N_{ifft} - 1$, in which it guarantees a power of 2 length for the input for IFFT block. The value of N_{ifft} depends on the LTE-Downlink bandwidth configuration. For example, in 20 MHz bandwidth configuration, $N_{ifft} = 2048$, $N_{sc} = 1200$ (for more information, see [1], and [10]).

We see the transmitted signal where PSS is supposed to be detected $s^1(n)$. On the other hand, when the $a_{k,l}$ does not contain the z_u, the received OFDM symbol does not have the synchronization signal which is the case when we name the signal by $s^0(n)$.

Now for defining the replica, we first define the $r_u(k') = [0, ...0, z_u, 0, ...0]$ with the length of N_{ifft}. Thus, applying the same IFFT formula, we have R_u as:

$$R_u(n) = R_u(nT_s) = \sum_{k'=0}^{N-1} r_u(k') . e^{j2\pi . k' . \Delta f . n . T_s} = \sum_{k'=0}^{N-1} r_u(k') . e^{j2\pi . k' . n/N} \tag{3.17}$$

[1]Note that the $a_{k',l}$ could be written as $a_l(k')$, but for following the notations in LTE standardization we use this notation.

Considering the above definitions, the cross-correlation follows equation (3.11). Now the probability of missing the symbol which contains the PSS is:

$$P_{miss} = P_r\Big(Q_u(n) < \gamma \Big| s_n^1\Big) \tag{3.18}$$

And probability of false alarm is:

$$P_{FA} = P_r\Big(Q_u(n) > \gamma \Big| s_n^0\Big) \tag{3.19}$$

where γ is a threshold. Usually P_{miss} and P_{FA} depend on the SNR of the received OFDM Symbol. The major factor in achieving the accurate sub-frame timing is P_{FA}. In next section, we use an algorithm that has a P_{FA} which does not depend on SNR. This is called Constant False Alarm Rate (CFAR).

3.3.2 CFAR and the proposed algorithm

As mentioned before, any miss in detecting the PSS sequence or the OFDM symbol which contains the PSS will cause waste of possible opportunity. On the other hand, probability of false alarm, will cause wrong timing information. This will result in both time and frequency overlap between SU and PU signals, as the scheduling at PU is taken place for every sub-frame. This is equal to waste of transmission resources for both PU and SU.

In the Neyman-Pearson framework, the probability of detection is maximized subject to the constraint that the false-alarm probability does not exceed a specified level. The false-alarm probability depends on the noise variance. Therefore, to calculate the false-alarm probability, we must first estimate the noise variance. If the noise variance changes, we must adjust the threshold to maintain a constant false-alarm rate. To avoid this situation, we need to have a limit for probability of false alarm. Constant False Alarm Rate (CFAR), is an algorithm in signal detection, which provides the

opportunity of having constant false alarm with respect to received signal SNR or SINR. Constant false-alarm rate detectors implement adaptive procedures that enable detector to update the threshold level when the power of the interference and/or noise changes. This means by using this algorithm, we expect constant false alarm rate for all values of received SNR.

We use the energy of the received signal as the adaptation parameter. So basically, we divide the square of the output of the correlator by the energy of the received signal. Then we can guarantee that the probability of the false alarm does not exceed a certain level. In [30], it is proven that in case of no frequency offset in sequence detection using correlation based methods, the probability of false alarm will be

$$P_{FA} = \Big(1 - \gamma\Big)^{L} \tag{3.20}$$

where L is the sequence length, and γ is the normalized threshold in percentage. According to above formula, the probability of false alarm will not exceed this level. It could be controlled by fixing the value of the threshold. The simulation shows similar result in the next section. For more information on how frequency offset will effect CFAR algorithm please see [30].

3.3.3 Simulation result for Probability of Miss and FA

The simulation below, evaluates the probability of miss and false alarm for detecting the PSS signal either with applying CFAR algorithm or without. The simulation parameters are presented in Table (3.2).

We choose 20 MHz bandwidth configuration of LTE-Downlink, and we modeled the channel as AWGN. We assume the $N_{ID}^{(2)}$ is known by detector, as it makes no difference in the analysis. The simulation shows the probability of miss and false alarm as a function of the threshold γ. We consider normalized signal energy, so the

Root index	$N_{ID}^{(2)} = 1$	$u = 29$
N.O. M-QAM sym. per OFDM sym	N_{sc}	1200
IFFT size	N_{ifft}	2048
Transmission Mod. Scheme	M-QAM	$M = 16$
Channel Model (Complex)	AWGN	—

Table 3.2: PSS Detection Simulation Parameters

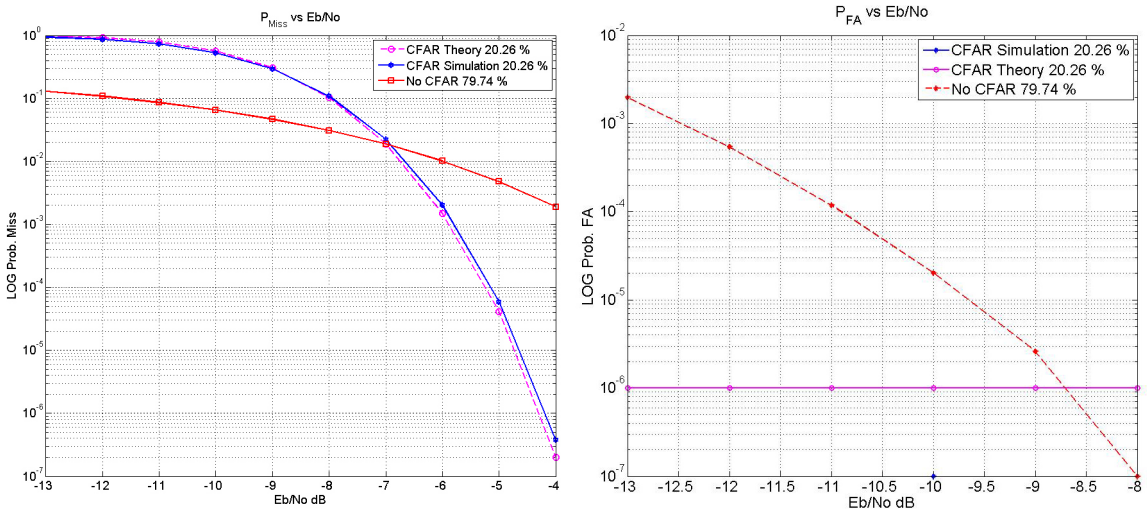

Figure 3.5: a) Probability of miss and b) false alarm, with respect to SNR, with and without applying CFAR algorithm for half frame observation

threshold should be chosen as a percentage of the energy of the PSS sequence.

In case of performing CFAR algorithm, as the received signal will be divided by its own energy, the level of the threshold should be chosen as a percentage of the energy of PSS sequence divided by the received signal energy. For simplicity in analyzing the figures, we present both methods (with and without CFAR) in Figure (3.5).

The probability of miss detection without performing the CFAR algorithm shows better performance in AWGN channel, only for E_b/N_o below -7 dB. Please note that in this stage of the work, probability of miss is only a delay in achieving sub-frame timing. On the other hand, the probability of false alarm causes wrong timing information, and consequently interference. Using the CFAR algorithm, the probability

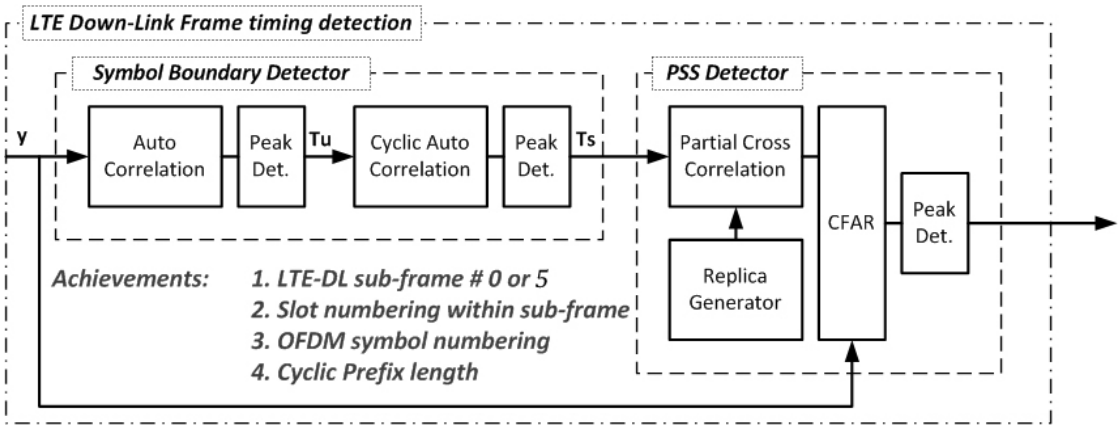

Figure 3.6: Overall sub-frame timing detection algorithm block diagram

of false alarm has taken constant value, which only depends on threshold γ. The typical values of E_b/N_o in sequence detection scenarios are usually varies from -7 to 0. This means, by using the CFAR algorithm we improve the probability of miss, while provide a guaranteed limit on the probability of false.

3.4 Summary

In this chapter we present a combined algorithm for achieving the sub-frame timing of an LTE Downlink signal, without having any prior knowledge of it. We evaluate the performance of the algorithm by finding the probability of miss detection of the PSS sequence by simulation. We applied CFAR algorithm for providing a guaranteed limit on the probability of false alarm. All the assumptions were based on the minimum tools available in sensor, for example no FFT processor at sensor. In short, the main purpose of this chapter was to evaluate the possibility of detecting the sub-frame timing of LTE signal by detecting the PSS.

The block diagram of the overall fame timing detection algorithm is provided in Figure 3.6. We consider blind detection of the LTE OFDM symbol boundaries. We consider a PSS detection algorithm based on cross-correlation function. having the

provided information from symbol boundary detection, the required processing load is reduced significantly. We improve the PSS detection by applying constant false alarm rate. The CFAR guarantees a limit on the probability of false alarm, which is the main cause of wrong timing detection, and consequently Interference between primary and secondary users.

As mentioned before, any miss detection in PSS detection process will cause waste of possible opportunity. On the other hand, probability of false alarm will cause wrong timing information, and will result in interference between SU and PU, which is the overlap in time and frequency. To avoid this situation, we need to have a threshold for probability of false alarm. Constant False Alarm Rate (CFAR), is an algorithm in signal detection, which provides the opportunity of having constant false alarm, i.e. independent of the SNR. According to the simulation result, applying CFAR algorithm not only provides a controllable false alarm rate, but also reduces the start up time of the Cognitive Sensing algorithm.

Chapter 4

Spectrum Hole Detection Algorithm

In the previous chapter we proposed a combined algorithm for obtaining the sub-frame timing of LTE-Downlink signal. In this chapter, we proposed a spectrum hole detection algorithm (SHD) which works based on frequency domain energy detection (in short we call it sensing). We use the timing information provided from previous chapter in order to start sensing at the beginning of each scheduling update. The sensing should be performed on the first data OFDM symbol. Then the decision made on the vacancy of the sensed symbols will be used for the rest of the symbols until next scheduling update. The detected time-frequency empty blocks are used for secondary transmission.

4.1 Overview of Sensing System

According to the user request, the eNodeB may assign from zero to several Resource-Block-Pairs (RBP) to each user. The scheduling is based on many parameters like the requested traffics and Channel Quality Indicator (CQI) feed-backs. The assigned RBPs to specific user could be attached together or interleaved in frequency domain.

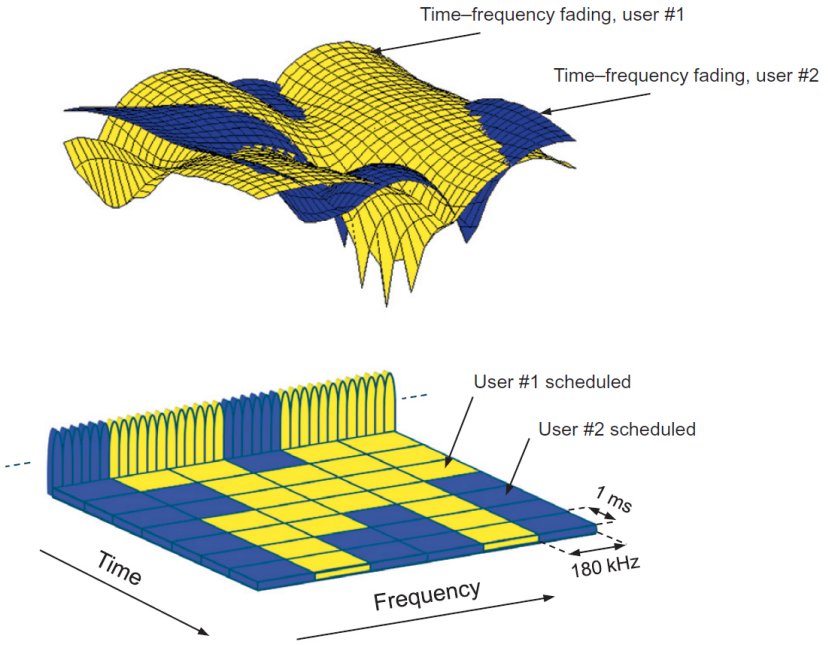

Figure 4.1: A Sample of Scheduling Decision in PU

In fact, they could have any distribution. Figure (4.1) shows how the resources are assigned to the users. However, it is possible that some of RBPs are not scheduled to any primary user, hence this is the main cause of underutilized resources. Figure (4.2) shows an example of resource grid illustration of LTE Downlink signal for the duration of 1^{ms} and bandwidth of 4 RBPs. Each RBP consists of 12 frequency sub-carriers for the duration of a sub-frame (1^{ms}). The first one, first two, or first three OFDM symbols (each OFDM symbol has around $71\mu s$) of a sub-frame are always filled by L1/L2 control information. In other words, the length of L1/L2 control information in time could be 1, 2, or 3 OFDM symbols. So basically there are two ways to investigate whether an RBP with a frequency band of 180 KHz and duration of $1ms$ is assigned to a user.

- The first way is to read the scheduling and channel assignment information which are transmitted at the beginning of each sub-frame within L1/L2 control symbols. The problem is that the control information is scrambled. They are

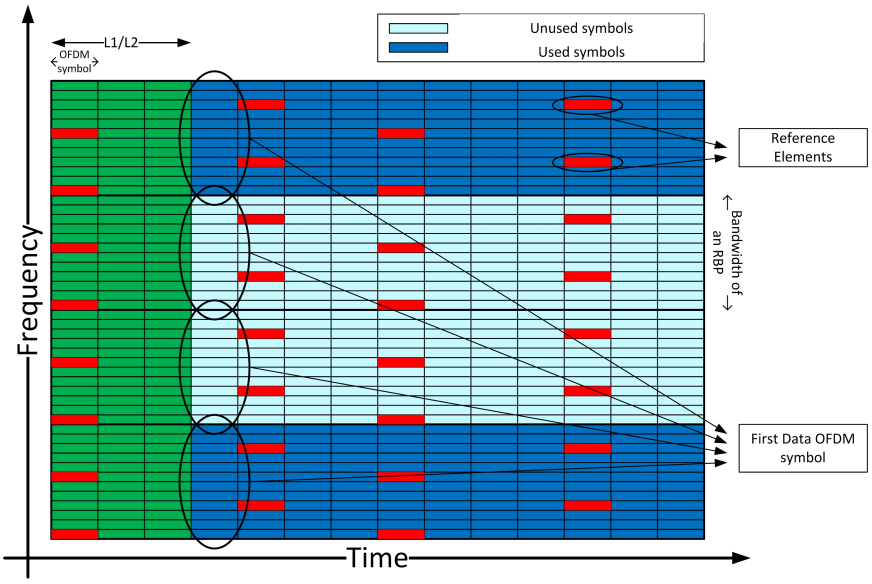

Figure 4.2: Resource Grid illustration of 4 RBPs (1^{ms})

not accessible for any user except the primary users equipment (UE) of the cell.

- The second way is to sense the energy of data OFDM symbols to find out whether or not the RBP is assigned to a user. In this case (which is the focus of this chapter) there is no need for decoding the scheduling information. On the other hand the sensor has to overcome other constraints. It should be well equipped to be able to perform all the required processes in appropriate time duration. Otherwise there would be not enough transmission time for the SU to communicate.

In general, the goal is to detect the energy of the first and/or second data OFDM symbols (following the L1/L2 control symbols). If the detected energy was below a certain value, the rest of symbols within the RBP is available for SU transmission.

4.1.1 Frequency Spectrum Energy Detector Requirements

The sensor requires knowing the beginning of each sub-frame. It also needs the OFDM symbol numbers l, from 1 to 14. Then it will be able to perform the energy detection

Processes	CPU Speed	Required Time
112640	778 GFLOPS	144.78 ns
112640	2000 GFLOPS	56.32 ns
112640	4903 GFLOPS	22.97 ns

Table 4.1: Required time for performing the FFT/IFT size 2048

on the first data OFDM symbol, which is following the L1/L2 control information. Based on the number of control OFDM symbols, the sensor may start sensing at $l = 3$, for the case of 2 control symbols, or $l = 4$ for the case of 3 control symbols.

The second requirement is that the sensor should be able to sense the energy of the specific frequency band of an RBP. Meaning that, the sensor should transfer the received OFDM symbol to frequency domain. In other words, the sensor requires taking the DFT of the received sampled signal, before starting to sense the energy of data symbols. For more accurate DFT/ FFT, knowing some parameters of the PU signal is beneficial. For example, being able to remove the CP of the signal will reduce the processing load, by reducing the FFT size. It also reduces the number of required multiplications for energy detection.

The last requirement is that the sensor should be able to perform the sensing process as fast as possible in less than 70 micro seconds. For example, if the SU transmission requires $0.5ms$ transmission with the bandwidth of $180KHz$, the sensing should make decision (on transmission on the specific RBP) in less than 300 μs. The faster the detection of available RBP is made, the higher the SU transmission rate is become.

4.1.2 Solution to the requirements

The answer for the first and second restrictions is given in Chapter 3. In Chapter 3, by detecting the boundaries of each OFDM symbol and also detecting the PSS, we provide the required information with high reliability.

For answering the last requirement, some examples of today's DSP processors are

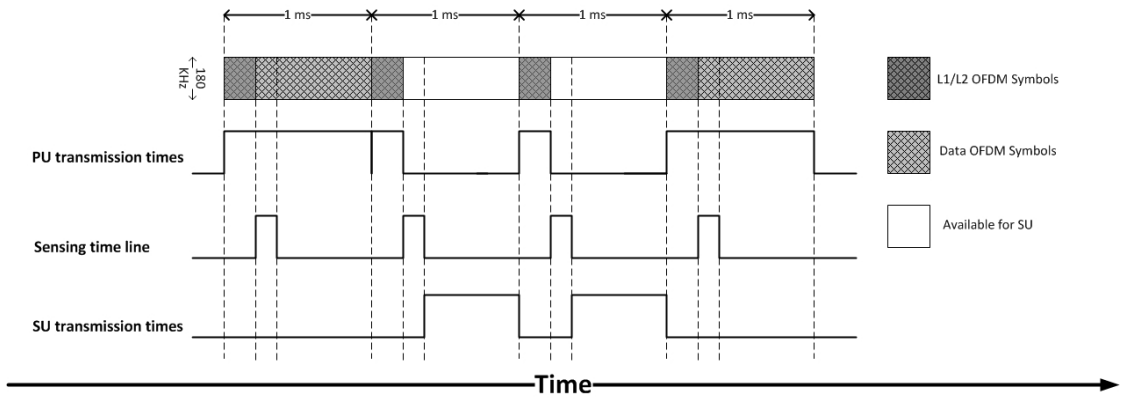

Figure 4.3: Time-line of the sensing and transmission

provided. It is shown that a typical DSP is able to perform all the required processes in much less time than the algorithm requires.

A survey on the existing processors

According to products introduction in [31], the Zynq-7000 DSP devices are able to perform up to 778 Giga-Floating-Points per Second. This number is increased to 2000 for 7 series of XILINX products, and to 4903 GFLOP/s in Ultra series. The amount of floating points required to perform an FFT or IFFT with the size of N, could be calculated as $5.N.log_2N$ [32]. As it is shown in table (4.1), considering $N = 2048$, the minimum required time for performing FFT varies from 145 to 23 ns. Note that the sampling rate of LTE is $32.5ns$. Thus, we provide a very generous time of $70\mu s$ for the sensor to calculate the energy of the OFDM symbol. Then the decision on the availability of the resource for secondary transmission is made. Figure (4.3) shows the time table of sensing and transmitting of the SU. The complexity discussion is provided only to evaluate the possibility of performing such a process.

4.2 System Model

In this section we provide the system model for the received signal, the channel, and the sensing algorithm. The decision making is based on comparing the received energy per band with a threshold level. The Threshold could be set according to a certain level of false alarm probability.

4.2.1 Signal Model

As the sensor doesn't have much information about the signal, Energy Detection (ED) is optimal in the Neyman-Pearson sense [33]. However, before characterizing the detection problem, we need to transfer the signal into frequency domain. Then we would be able to measure the energy of the symbols for a specific bandwidth. That is, to take the DFT of the sampled received signal. The transmitted signal model is:

$$s(n) = s(nT_s) = \sum_{k'=0}^{N-1} a_{k',l}.e^{j2\pi.k'.\Delta f.n.T_s} = \sum_{k'=0}^{N-1} a_{k',l}.e^{j2\pi.k'.n/N} \tag{4.1}$$

where $a_{k',l}$ is M-QAM symbol transmitted within l^{th} OFDM symbol. M could be 4, 16 or 64 depending on Channel Quality Indicator (CQI) and Adaptive Modulation and Coding scheme (AMC). Equation (4.1) is the inverse discrete Fourier transfer and the Δf is sub-carrier spacing. k' is the number of sub-carriers from 0 to $N_{RB}.N_{sc}^{RB} - 1$. T_s is sampling rate as described in Chapter 2. Note that here N is N_{ifft}.

On the sensor side, $y(n) = s(n) + w(n)$ is the input of the FFT block, and $w(n)$ is Additive White Gaussian Noise. Note that $s(n)$ is the LTE-Downlink transmitted OFDM signal. At the spectrum hole detector, the symbols are modeled as:

$$\hat{a_{k',l}} = \sum_{n=0}^{N-1} y(n).e^{-j2\pi.k'.n/N} \tag{4.2}$$

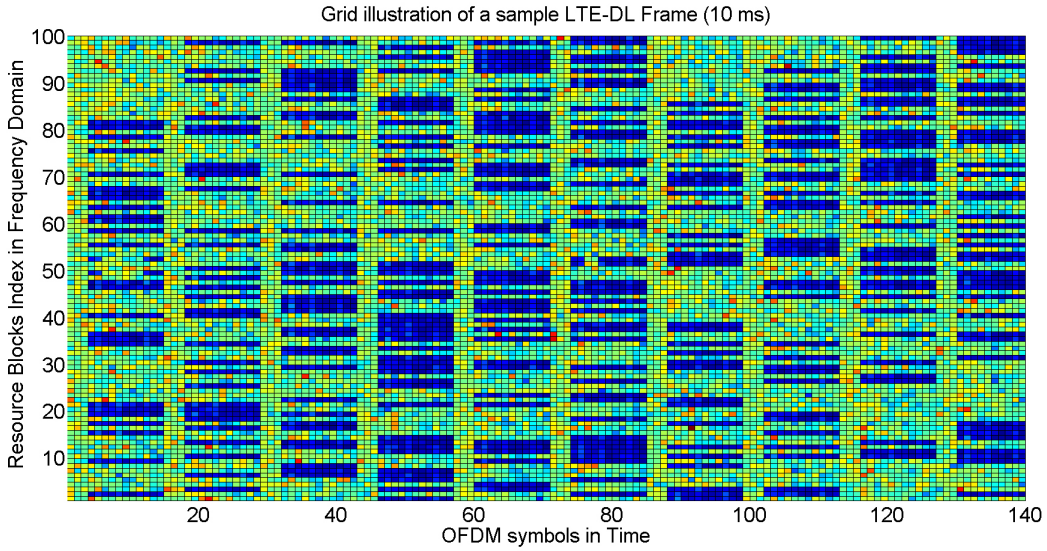

Figure 4.4: Resource Grid illustration of LTE-DL Frame in presence of noise

where $y(n)$ is the sampled received OFDM symbol. Equivalent to what we had for $y(n)$, we could say $a_{\hat{k'},l} = a_{k',l} + z(k)$. Figure (4.4) shows a simulated example of resource grid illustration of received signal for the duration of one frame ($10ms$). The bandwidth configuration is 20 MHz consists of 1000 RBPs. In this bandwidth configuration, the signal consists of 1200 sub-carriers, and the IFFT size is 2048. The bandwidth of 12 sub-carriers is the bandwidth of a resource block, which is $180KHz$. So the Figure (4.4) shows 18 MHz bandwidth for 10 ms (1 MHz guard-band at each side). The equation (4.1) and (4.2) are considering total sub-carriers of the LTE Downlink frequency bandwidth. LTE has flexible bandwidth configuration from 1.4 MHz (6 RBP or 71 sub-carriers) to 20 MHz (100 RBP, 1200 sub-carriers). For simplicity in notation marks, from now we only consider the bandwidth of an RBP (180 KHz) consists 12 sub-carriers. Then we define k from 0 to 11, instead of k'. We say an RBP, has the potential to be used for SU transmission, only if the related $a_{k,l}$ is zero.

4.2.2 Sensing Model

Now consider $\widehat{a_{k,l}}$, as received data symbols within the l^{th} OFDM symbol. The binary hypothesis is showing the availability of the RBP for transmission of the secondary user:

$$\begin{cases} H_0: & \widehat{a_{k,l}} = z(k), & \textit{Related RBP is not assigned to any PU} \\ H_1: & \widehat{a_{k,l}} = a_{k,l} + z(k), & \textit{Related RBP is assigned to a PU} \end{cases}$$

where $k = \{0, \ldots, 11\}$ is sub-carrier index per resource block pair (RBP). Here $z(k)$ is zero mean Gaussian random variable and $a_{k,l}$ is the M-QAM symbol with normalized average energy equal to one. The $\widehat{a_{k,l}}$ values are 12 observed samples for each RBP, consists of normalized energy M-QAM symbols $a_{k,l}$, and zero mean complex Gaussian random variables with variance σ_z^2 per dimension. The Neyman-Pearson detector is a threshold detector on the likelihood ratio or equivalently the log-likelihood ratio (LLR):

$$LLR = log\left(\frac{p(\widehat{a_{k,l}}|H_0}{p(\widehat{a_{k,l}}|H_1)}\right) \gg\ll \gamma' \tag{4.3}$$

where γ' is the suitably chosen threshold. Given the independent and identical assumption, the detector is easily seen to be equivalent to deciding H_1 if

$$E = \frac{1}{2N_{sc}^{RB}\sigma_z^2}\sum_{k=0}^{11}|\widehat{a_{k,l}}|^2 > \gamma \tag{4.4}$$

The statistic E is a scaled version of a standard χ^2 random variable with $2N_{sc}^{RB}$ degrees of freedom. where N_{sc}^{RB} is the number sub-carriers to be observed at each RBP. For example if the sensor senses two adjacent data OFDM symbols, the degree of freedom become 48. The simulation is performed on sensing only 1 data OFDM symbol. We next evaluate the ROC for the Energy Detector.

ROC of Energy Detector

If x_i are independent real Gaussian variables with zero means and unit variance, then

$$x = \sum_{i=1}^{2N_{sc}^{RB}} x_i^2 \tag{4.5}$$

is χ^2 distributed probability density function (pdf) of ([12] section 4.2):

$$p(x) = \frac{1}{2^{N_{sc}^{RB}}(N_{sc}^{RB}-1)!} x^{N_{sc}^{RB}-1} exp(-\frac{x}{2}) \tag{4.6}$$

The tail probability $Pr(x > \gamma)$ is computed via integration by parts as:

$$\begin{aligned} \Pr(\mathrm{x} > \gamma) &= \int_{\gamma}^{\infty} \frac{1}{2^{N_{sc}^{RB}}(N_{sc}^{RB}-1)!} x^{N_{sc}^{RB}-1} exp(-\frac{x}{2}) dx \\ &= \mathrm{e}^{-\gamma/2} \sum_{k} \frac{1}{k!} \Big(\frac{\gamma}{2}\Big)^{k} \\ &= \Gamma_u(\gamma/2, N_{sc}^{RB}) \end{aligned} \tag{4.7}$$

where $\Gamma(\cdot,\cdot)$ is the upper incomplete gamma function defined by

$$\Gamma_u(a,n) = \frac{1}{\Gamma(n)} \int_a^{\infty} x^{n-1} e^{-x} dx \tag{4.8}$$

Now the test statistics $E \times 2N_{sc}^{RB}$ has the same pdf as a χ^2 variable with $2N_{sc}^{RB}$ degrees of freedom. hence, the probability of false alarm P_{FA} and the probability of miss detection P_M for the energy detector can be obtained as [12]

$$P_{FA} = \Gamma_u(N_{sc}^{RB}\gamma, N_{sc}^{RB}) \tag{4.9}$$

$$P_M = 1 - \Gamma_u\Big(\frac{N_{sc}^{RB}\gamma}{1+snr}, N_{sc}^{RB}\Big) \tag{4.10}$$

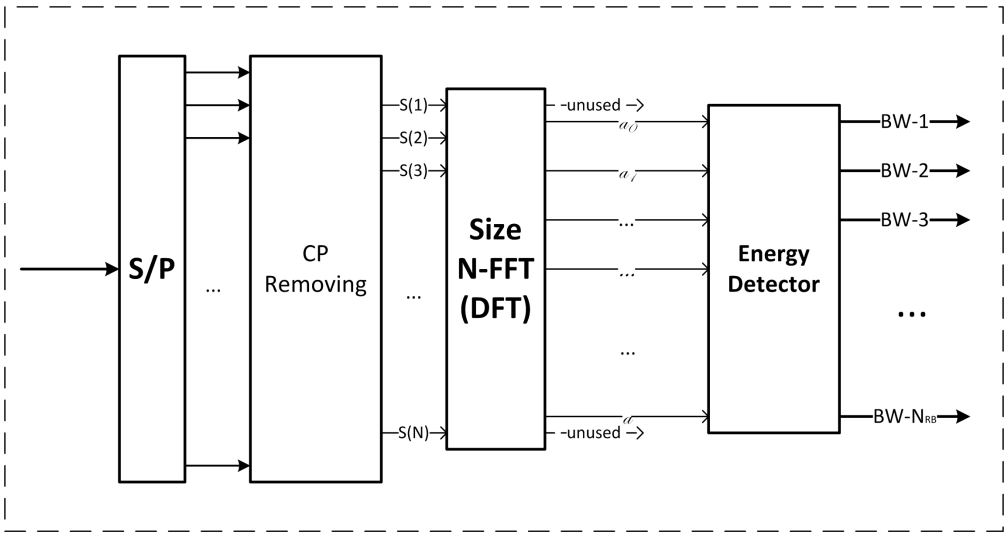

Figure 4.5: Block diagram of LTE-DL spectrum hole detector

As seen, one disadvantage of the energy detector is that at low SNR the number of samples required to achieve specified performance is proportion to $1/snr^2$.

4.3 Energy Detection Algorithms

For being able to detect the energy of the samples within the bandwidth of each resource block pair, we should transfer the received OFDM symbol to frequency domain. Then for each bandwidth, we have 12 samples for the duration of an OFDM symbol. The Figure (4.5) shows the block diagram of the frequency domain energy detector. The FFT is performed on each received OFDM symbol. The energy detector calculates the energy of each bandwidth for the first (or the first and second) data OFDM symbol of each sub-frame. Then by comparing the calculated energy with a threshold, the decision on the availability of the rest of sub-frame on each bandwidth is made. For simplicity, we analyze the performance of the algorithm for the bandwidth of only one RBP.

Now consider the case where the energy detector treated the component $a_{k,l}$ as the mean of the received signal under H_1. Then, each $\widehat{a_{k,l}}$ is Gaussian with mean $a_{k,l}$

and variance σ_z^2. The P_{FA} for ED is given by equation (4.9) as before. Under the H_1, E is non-central χ^2 distribution with $2N_{sc}^{RB}$ degrees of freedom. By defining the non-centrality parameter as:

$$\mu^2 = \frac{1}{2N_{sc}^{RB}\sigma_z^2}\sum_k |a_{k,l}|^2. \tag{4.11}$$

The probability of detecting the energy $P_D = Prob(E > \gamma|H_1)$, is given by tail probability ([34], [7], and [33]) of this distribution, which has been expressed as:

$$P_D = Q_n(\mu, \sqrt{2N_{sc}^{RB}\gamma} \quad) \tag{4.12}$$

where $Q_n(a, b)$ is generalized Marcum Q function,

$$Q_n(a, b) = \frac{1}{a^{(n-1)}}\int_b^\infty x^n exp(-\frac{x^2 + a^2}{2})I_{n-1}(ax)dx \tag{4.13}$$

where I_n is the modified Bessel function of the first kind, of order n. Note that the mean and variance of E are given by $1 + \mu^2$ and $(1 + 2\mu^2)/n$. For large number of samples, the central limit theorem can be invoked and the ROC can be achieved via Gaussian approximation. Further, evaluation of the performance of the ED requires knowledge only of the SNR and the parameter μ. This corresponds to a special case of the Bayesian linear model discussed in [33].

4.4 Simulation Results

The performance of the ED is evaluated in terms of Probability of Miss Detection and Probability of False Alarm. A $20MHz$ bandwidth configuration for LTE-Downlink signal is considered. This is equal to the transmission of near 1200 data symbols for the duration of 1 OFDM symbol within this bandwidth. Each 12 of these data

Number of sc per RB	N_{sc}^{RB}	12
Number of RB per sub-frame	N_{RB}	100
IFFT size	N	2048
Transmission Mod. Scheme	M-QAM	$M = 4, 16$
Channel Model (Complex)	AWGN	—

Table 4.2: SHD Simulation Parameters

symbols has the bandwidth of $180KHz$ ($12\times15KHz$), and consider as the bandwidth of an RB[1]. Table (4.2) shows the configuration of the signal.

According to ROC discussion, the degree of freedom, for sensing 1 OFDM symbol per RBP, is $2N_{sc}^{RB} = 24$,. Considering the variance of E given by $1+\mu^2$, the probability of miss detection for different threshold γ is shown in Figure (4.6).

$$P_{miss} = P_r\Big(E < \gamma\Big|H_1\Big) \tag{4.14}$$

Note that missing the energy of an RBP at the beginning of its transmission causes interference between SU and PU in that specific bandwidth. For simulating the probability of false alarm we need to calculate E at H_0 according to equation (4.4):

$$E\Big|_{H_0} = \frac{1}{2 * 12 * \sigma_z^2}\sum_k |\widehat{z(k)}|^2 \tag{4.15}$$

Then it takes the constant value equal to equation (4.9). The simulation result is shown in Figure (4.7). The constant value of the false alarm with respect to SNR, is because of the normalized received signal energy with the variance of the noise. Note that, the probability of successfully detecting the spectrum hole (bandwidth of an RBP) is the probability[2] of having the detected energy level below the threshold given H_0.

$$P_{HD} = P_r\Big(E < \gamma\Big|H_0\Big) = 1 - P_r\Big(E > \gamma\Big|H_0\Big) = 1 - P_{FA} \tag{4.16}$$

[1]Note that the bandwidth of a resource block is equal to the bandwidth of resource block pair, as they are paired in time.

[2]HD stands for spectrum Hole Detection.

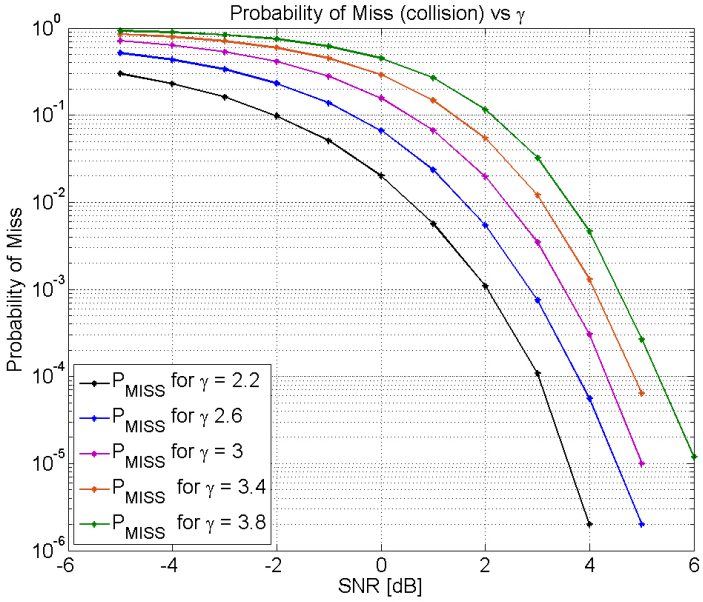

Figure 4.6: Probability of Miss Detection with respect to SNR for different γ

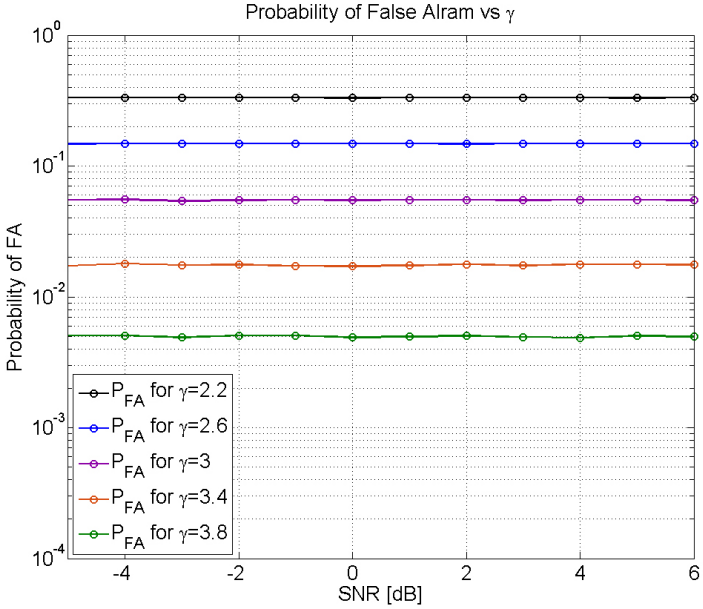

Figure 4.7: Probability of False Alarm with respect to SNR for different γ

There is a trade off between producing interference for the PU (P_{miss}), and wasting an opportunity (P_{FA}). Fortunately, by setting a limit for the probability of false alarm, one may choose the proper value of threshold, while considering the operating SNR.

4.5 Conclusion

In this chapter, we evaluate a sensing algorithm which is based on frequency domain energy detection. The algorithm senses the availability of every Resource Block Pair by detecting the energy of the beginning of it. This method is a dynamic real-time sensing algorithm which enables the SU to fill upto 82% of the underutilized resource block pairs. With the aid of this algorithm, we eventually are able to sense and search the spectrum holes within the LTE-Downlink signal. The advancements in designing processors is a key parameter, and it enables the sensor to perform the required functionality within appropriate time. The performance of the energy detector in AWGN environment is evaluated in both theory and simulation. The probability of false alarm is causing the waste of an opportunity for the SU transmission. On the other hand, the probability of missing the available energy on a specific bandwidth will cause the wrong detection of spectrum hole. This is equal to the probability of imposing interference to the PU signal. Therefore, the trade off between the possible limit of interference and waste of opportunities should be configured by choosing a proper threshold. As the probability of false alarm is only the function of threshold, one may choose a threshold level in a way for neither experiencing too much of waste of transmission opportunities, nor producing much interference.

Chapter 5

System Evaluation

In this chapter, we first present a wireless transmission scheme, which is capable of operating in the real-time secondary spectrum access scenario[1]. The Cognitive Sensing algorithm provides the available frequency bands for the transmission of the secondary user at each scheduling update, while the transmission scheme is cable of configuring the frequency band of its transmission signal very fast. This means the the Cognitive Sensing algorithm is independent of the primary user traffic model, distribution of the PU's active end users both in time and frequency, and also the activity factor of primary user.

In the second part of this chapter, we assume that any collision between SU and PU blocks cause the complete lost of the packet. We statistically evaluate the rate loss at the primary user side, and also the average value of the achieved data rate at the secondary user side. The bandwidth utilization of the system is also compared to the case when the Cognitive Radio Network solution is not employed. Considering the developed cognitive Sensing algorithm, the whole system is capable of utilizing upto 82% of the underutilized bandwidth.

[1] As described in Chapter 2

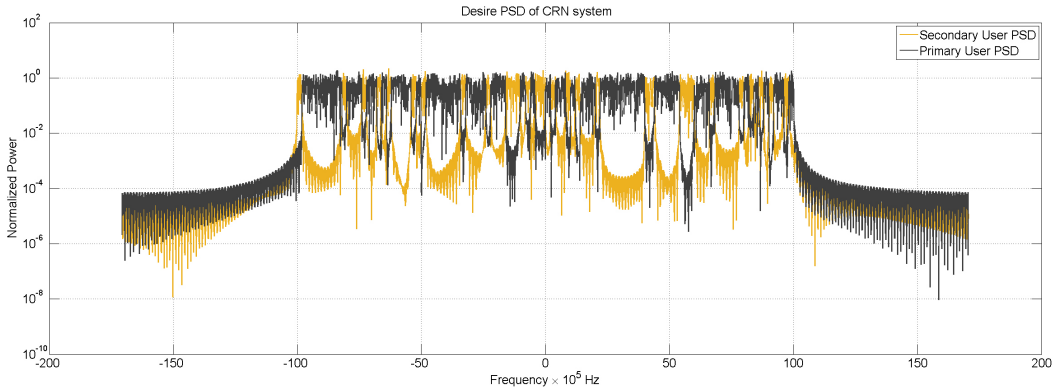

Figure 5.1: The utilization of non-contiguous regions of frequency spectrum by secondary user signal

5.1 Cognitive Radio Transmission Scheme

In Figure 5.1, we illustrate the expected Power Spectral Density (PSD) of primary and secondary signals, operating in the Secondary Spectrum Access (SSA) scenario. The SSA is the promising solution to the artificial spectral scarcity problem described in Chapter 1. At any time instance, several non-contiguous frequency bands are left unused. By ensuring that the primary user's rights are not violated, these unused portions can be used by secondary users. In Chapter 3, and 4 we developed an algorithm for detecting these frequency portions at the beginning of their life span, and named it **Cognitive Sensing**. Now we present some characteristics of a transmission scheme which fits to both cognitive sensing algorithm and primary user transmission standardization.

5.1.1 Underlay or Overlay Transmission

As discussed in Chapter 2, spectrum sharing techniques can be classified into *underlay* and *overlay* spectrum sharing based on the spectrum access techniques. Underlay systems use ultra-wide-band (UWB) [35], [36] or spread-spectrum techniques, such as code division multiple access (CDMA) [37], to transmit the signal below the noise floor

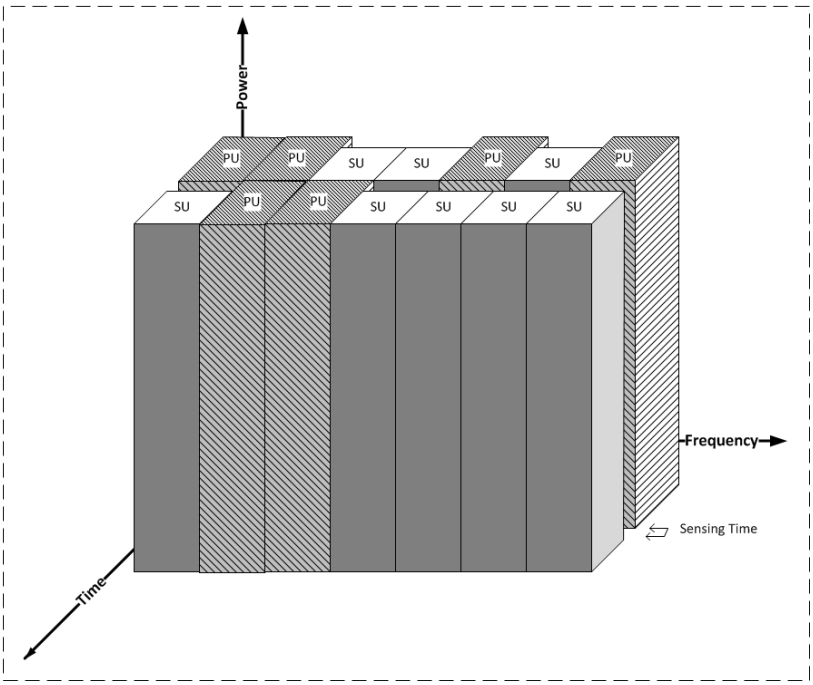

Figure 5.2: Illustration of our Overlay Cognitive Scenario.

of the system [38]. However, this technique can increase the overall noise temperature and thereby, worsen error robustness of the primary users as compare to the case without underlay systems. In [39] the notching, and in [40] waveform adaptation interference avoidance techniques for underlay scheme are presented.

Now consider the case when the spectrum holes (an unused portion of the licensed spectrum [15]) are filled with the transmission of secondary user, i.e. the overlay technique. It has been shown that frequency division multiplexing is an optimal technique, when interference among the users is high [41]. As shown in the Figure (5.2), the overlay system uses the unoccupied portion of the frequency spectrum for the secondary user transmission. Since the licensed system has privileged access to the spectrum, it must not be disturbed by any secondary transmissions.

In [42] two main design goals for an overlay system are defined as:

- Minimum interference to licensed transmission.
- Maximum exploitation of the gaps in both time and frequency domain.

Therefore, the overlay system requires information about the spectrum allocation of the licensed system. This information could be available either by using a sensing algorithm (real-time secondary spectrum access), or by having access to a data base (Spectrum pooling[2]). However, the scenario in this work requires a real-time access. The proposed cognitive sensing algorithm provides this information in a real-time manner, while the overlay system is capable of exploiting the unused portion of the spectrum neither by interfering with the incumbent users nor by increasing the noise temperature of the system. So, the chosen secondary transmission scheme should follow the overlay system.

For having a successful coexistence in the overall bandwidth between primary and secondary users, the overlay system should not degrade the performance of the system already working in the neighboring frequency bands (i.e. LTE-Downlink Signal). For instance, out-of-band radiation has to be reduced to enable coexistence. Several approaches have been proposed in literature for suppressing the side lobe levels, such as the deactivation of sub-carriers lying at the borders of an OFDM spectrum [44], windowing [45], sub-carrier weighting [46], and insertion of cancellation carriers [47].

5.1.2 Non-Contiguous OFDM Transmission

Despite being a solution to the problem of the apparent spectrum scarcity, Dynamic Spectrum Access (DSA) puts additional design constraints on the wireless transceiver. As multiple bands of wireless spectrum are being utilized, the noise characteristics differ substantially across the non-contiguous bands of spectrum. Hence, the wireless transceivers employed in DSA technique, requires to use the spectrally agile but extremely robust modulation technique. As mentioned earlier, the non-contiguous OFDM proposed in [48] satisfies these requirements. While conventional multi-carrier (MC) CDMA has proven to be effective compared to conventional OFDM systems

[2]For information on Spectrum Pooling read [43]

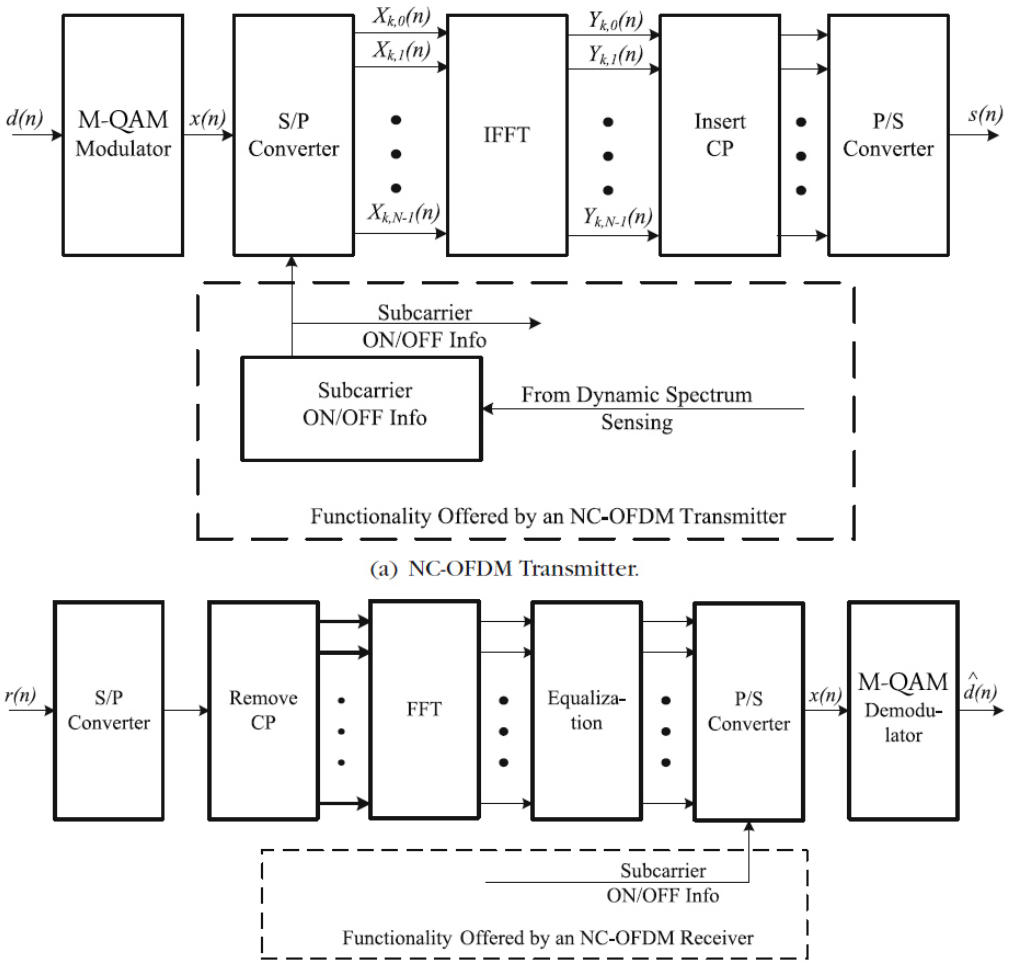

Figure 5.3: An NC-OFDM transceiver.

because of its superior multi-user interference limiting capabilities, NC-OFDM has been shown to be better than non-contiguous MC-CDMA (NC-MC-CDMA) [49]. This is because the deactivation of subcarriers corresponding to primary-user transmissions causes a loss of orthogonality in NC-MC-CDMA, leading to a worse bit error rate (BER) performance than NC-OFDM systems. Therefore, our focus for spectrally agile modulation techniques is NC-OFDM.

Structure

Figure (5.3) shows a general schematic of a NC-OFDM transceiver. Without loss of generality, a high speed digitally modulated (M-PSK, M-QAM) data stream, $x(n)$ is split into N slower data streams using serial-to-parallel (S/P) converter. Note that unlike the conventional OFDM scheme, sub-carriers correspond to underutilized RBPs are activated for SU transmission, while the other sub-carriers are deactivated for interference prevention. The cyclic prefix insertion and other blocks follow the conventional OFDM scheme. The baseband NC-OFDM $s(n)$, is passed through the transmission radio frequency chain, which amplifies the signal and up-converts it to the desire center frequency. Note that, in this chapter we refer $s(n)$ as secondary user transmission signal.

At the other side, the receiver performs the reverse operation of the transmitter. First, by mixing the RF signal to the baseband for processing, and yielding the signal $r(n)$. Then, the signal is converted into parallel streams using the S/P converter, the CP is removed, and the FFT is applied. After compensating distortion introduced by the channel using equalization, the data in the active subcarriers are multiplexed using a P/S converter, and demodulated into a reconstructed version of the original high-speed input, $\widehat{x(n)}$.

Some of the design constraints associated with such a secondary user transceiver scheme are spectrum shaping , peak to average power ratio, and the FFT pruning. The closed discussions on these issues are provided in Chapter 6 of [12], and is out of the scope of this work.

We have presented the non-Contiguous OFDM scheme as the secondary user transmission technique. This scheme could be seen as a very close one to the primary user downlink technique. Considering same sub-carrier spacing, and similar resource grid structure, we are able to evaluate the performance of the proposed Cognitive Sensing algorithm in terms of Data Rate, and Bandwidth Utilization. We assume the

transmission of SU signal on any in-use RBP will cause complete drop (we call it collision). Based on this assumption, we evaluate the overall performance using the simulation results of previous chapter. The activation factor of the primary user, β plays a critical role in the gained data rate at SU side and also in the percentage of improvement in total system bandwidth utilization.

5.1.3 Consideration in Secondary User Transmission Scheme

In LTE Downlink signal there are many pilots transmitted among data symbols. The location of those pilots is known in resource grid illustration of LTE Downlink signal while the timing information is obtained. However, it is worthy to mention that if the secondary user transmits within a detected available block, it should consider not to impose any interference to those pilot signals. The location of the pilots in time and frequency is very well defined in LTE standardization.

As an example of the pilot signals, we could mention the PSS or SSS sequences which are transmitted periodically within LTE Downlink signal. The location of this signal is known for the sensor. Thus the secondary user transmitter should avoid to transmit within those location.

5.2 Interference Caused by SU

In this section, we consider the scenario in which the LTE-Downlink is impaired by SU signal due to wrong detection of an RBP as an underutilized resource. Of course there are other possible interference scenarios like spectral leakage and side-lob emissions. They are very well investigated in [24], and [23], and we refer the interest readers to those works.

5.2.1 System Model

Consider an LTE system operates in FDD mode with bandwidth configuration of 20 MHz. There are 100 resource block pairs available for channel assignment of each sub-frame. If we grant the activation factor of β to primary user, in average there would be $(1-\beta)$ underutilized resource available for the SU.

Now consider the case when the Cognitive Sensing algorithm fails to detect the PU signal energy. This is equal to have collision between SU and PU, and may happen with the probability of miss detection in Chapter 4. For simplicity in notations we donate the q to the probability of miss detection of primary user signal in a specific resource block pair.

On the other hand, the correct detection of an RBP, with the probability[3] of p leads to successful transmission of data at SU side. Summarizing the above definitions, we have:

1. β : Activation factor of primary user.
2. q : Probability of having collision due to wrong detection of a spectrum hole.
3. p : Probability of correct detection of spectrum hole, and successful secondary user transmission.

before starting the evaluation, we need to review the secondary user sensing and transmission procedure.

Secondary User Operation Procedure

Consider the bandwidth of and RBP for the duration of two-millisecond, i.e two RBPs. As shown in Figure (5.4), the first RBP is not assign to any primary user, but the second one is assigned. As mentioned in Chapter 4, it takes up to two OFDM symbol duration for the energy detector, to check the availability of primary data

[3]This is equal to probability successful detection of un-used RBP in Chapter 4, P_{HD}.

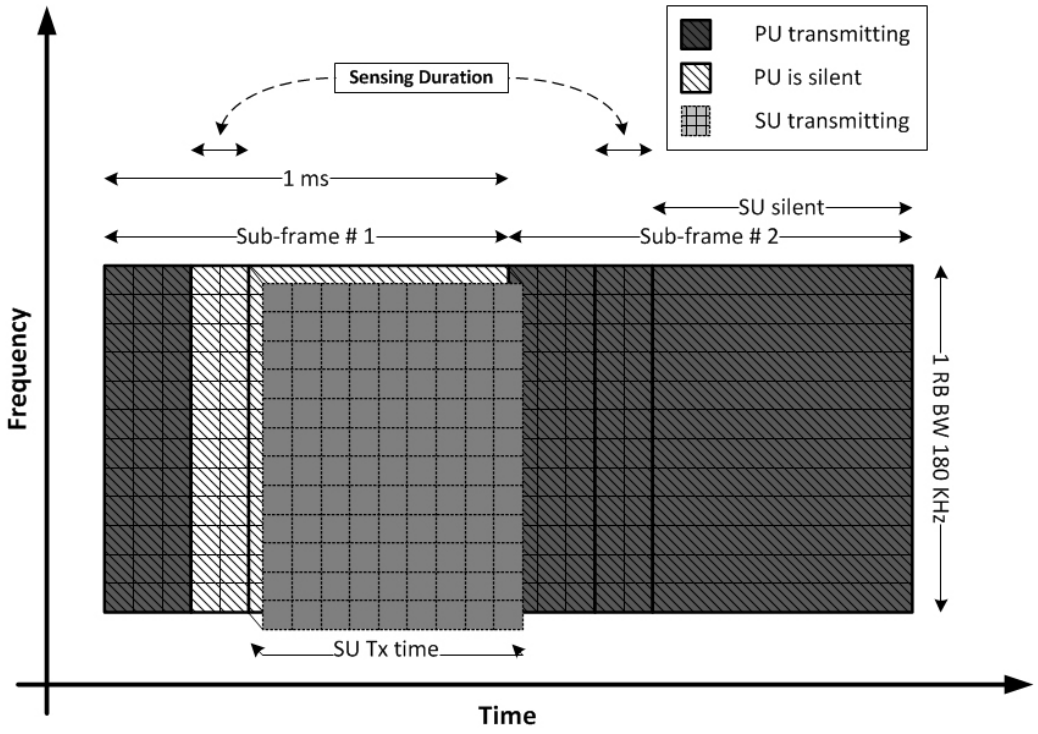

Figure 5.4: Time-Frequency illustration of Cognitive transmission for 1 RBP.

symbols in that specific bands. Considering maximum of three OFDM symbol for L1/L2 control information of LTE, the available time-frequency grid for secondary transmission consists of N_{SU} data symbols per detected resource block pair.

$$N_{SU} = N_{sc}^{RB} \times (N_{symb} - N_{symb}^{L1/L2} - N_{symb}^{sensing}) \quad data\ symbols\ per\ RBP \tag{5.1}$$

where N_{sc}^{RB} is the number sub-carriers per bandwidth of resource block[4], N_{symb} is the number of OFDM symbols per sub-frame which is 14, while the $N_{symb}^{L1/L2}$ and $N_{symb}^{sensing}$ are number of OFDM symbols dedicated to L1/L2 and required for sensing algorithm, respectively. So the $N_{SU} = 12 \times (14 - 3 - 2) = 108$ data symbols per RBP.
This is, while the primary user transmits $N_{PU} = 12 \times (14 - 3) = 132$ data symbols per RBP in this configuration. So by simply comparing the N_{SU} and N_{PU}, the maximum achievable bandwidth utilization improvement is 81.81%.

[4]Bandwidth of RB is equal to that of RBP

We assume, any collision between secondary and primary user will cause complete drop of N_{PU}. So by having the probability of collision we could calculate the Primary user data rate loss.

5.2.2 Primary Rate Loss due to Interference caused by SU

Assuming the Cognitive Sensing algorithm spends enough time on start-up, i.e. obtaining error free primary user sub-frame timing. The secondary user transmits on a specific RBP under two conditions:

- The RBP is inactive, and the SU correctly detect it. Then the probability of being in this condition is $(1-\beta).p$.
- The RBP is active, and the SU has missed to detect its energy. So the probability of this case is $P_I = \beta.q$.

where P_I, is probability of interference caused by SU for a specific RBP. Then the probability of SU produce interference for at least one of the RBPs among all 100 RBPs of PU signal is:

$$Pr = 1 - (1 - P_I)^L \approx P_I.L, \quad L = 100 \tag{5.2}$$

This is the probability of SU having at least one collision with one of the RBPs within 20 Mhz of bandwidth and one-millisecond of PU transmission. Now the Data Rate Loss due to the interference caused by SU wrong detection is calculated as:

$$R_{PU}^{Loss} = R_{PU}^{RBP} \times Pr \quad symbols\ \ per\ \ second \tag{5.3}$$

where R_{PU}^{RBP} is the amount of data rate that primary user can transmit in a bandwidth of an RBP:

$$R_{PU}^{RBP} = N_{PU} \times 1/1^{ms} \quad symbols\ \ per\ \ second \tag{5.4}$$

Threshold γ	$q = P_{miss}$	R_b^{Loss}
2.2	2×10^{-6}	36.96 bps
2.4	1×10^{-5}	151.2 bps
2.6	5.8×10^{-5}	1.07 kbps
3	3×10^{-4}	5.5 kbps
3.4	1.3×10^{-3}	24 kbps
3.8	4.3×10^{-3}	79.4 kbps

Table 5.1: Numerical Result of the Rate Lost at PU for SNR = 4 [dB]

Then the equation (5.3) is reduced to:

$$R_{PU}^{Loss} = N_{PU} \times 1/1^{ms} \times P_I.L = 132 \times 10^3 \times 100 \times \beta.q \tag{5.5}$$

As an example, consider the $\beta = 70\%$, and QPSK modulation, each data symbol will translate to two bits. Then the lost bit rate could be calculated according to the simulation results for q, in Chapter 4.

This means, if the probability of missing the PU signal and producing interference for that is e.g. $q = 10^{-5}$, and assuming the collision will cause complete lose, also considering activity factor of $\beta = 70\%$, the average total bit rate that PU is losing within all its 20 MHz bandwidth is $R_b^{Loss} = 151.2$ bps, according to equation (5.3) or (5.5).

5.2.3 Secondary Data Rate Gained

Correct detection of an RBP as the available transmission resource for secondary user means the improvement of bandwidth utilization of the system. Considering equation (5.1), the transmission data rate at the SU per RBP is:

$$R_{SU}^{RBP} = N_{SU} \times 1/1^{ms} \tag{5.6}$$

Threshold γ	P_{FA}	R_b^{SU}
2.2	3×10^{-1}	4.5 Mbps
2.6	1.5×10^{-1}	5.5 Mbps
3	5×10^{-2}	6.15 Mbps
3.4	1.8×10^{-2}	6.36 Mbps
3.8	5×10^{-3}	6.447 Mbps

Table 5.2: Numerical Result for Rate Gained by SU

Following the same attitude of previous section, the average data rate gained at secondary user side within the whole 20 MHz bandwidth could be calculated as:

$$R_{SU} = R_{SU}^{RBP} \times L.(1-\beta).p \tag{5.7}$$

Assuming the same modulation order, and β value, using the simulation results from Chapter 4, the Table (5.2) shows numerical results for average bit rate at SU transmission. Note that the primary user activation factor plays the main role in upper bound of achievable data rate. Maximum achievable data rate is always less than $1-\beta$.

5.2.4 The Bandwidth Utilization of the Overall system

We evaluate the Bandwidth Utilization η, with respect to activation factor of primary user β. We normalize the η to the case when the primary user utilized all resources, i.e. the activation factor is 100%. In this case the secondary user transmission fall to zero. Figure (5.5) shows the bandwidth utilization improvements at the sensor operating point of $\gamma = 2.2$, and the received SNR at the sensor $SNR = 4dB$. Considering AWGN channel between secondary user transmitter and receiver, and 4 dB signal to noise ratio, upto 81.81% of the underutilized resources could be occupied, at each one-millisecond. Obviously at lower SNR and threshold values which cause more collisions, this performance degrades. The Figure (5.6), shows the Bandwidth Utilization of the system with respect to E_b/No for two different β values. As mentioned, the simulation

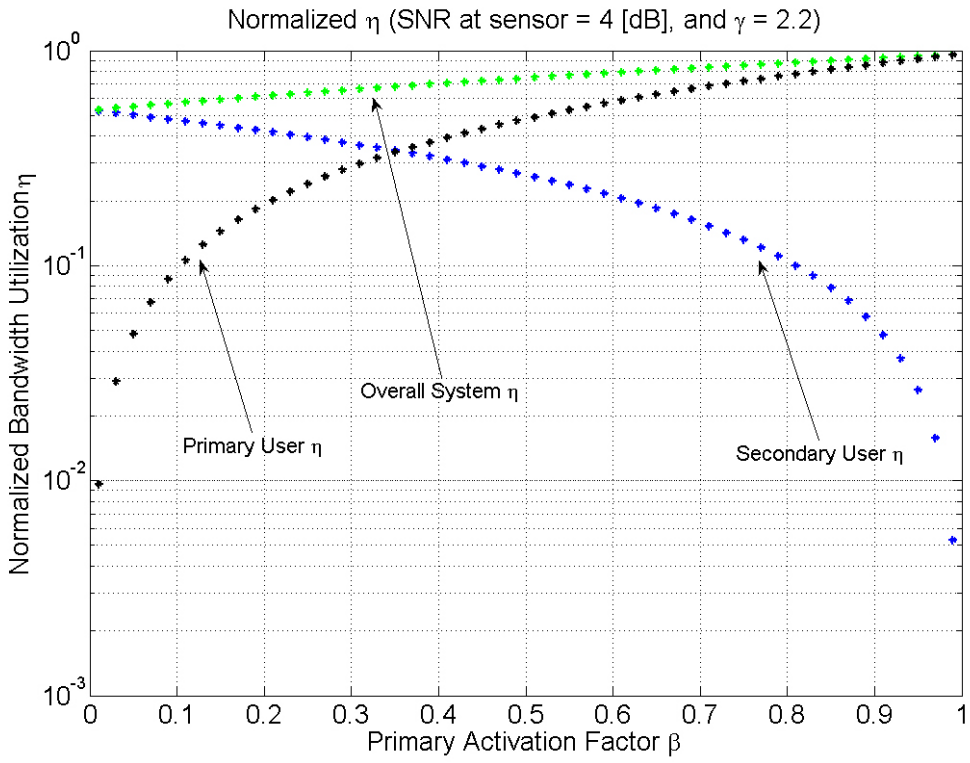

also considers the bit error rate for the same value of received SNR, in AWGN channel, in calculating the normalized bandwidth utilization.

5.3 Conclusion

In this chapter, we suggest the NC-OFDM transmission scheme for the proposed Cognitive Sensing algorithm. This scheme is very close to LTE Downlink transmission, and the difference is that the sub-carriers correspond to an RBP could be activated for transmission or not. If the parameters of NC-OFDM, such as sub-carrier spacing and OFDM symbol duration, are chosen to be equal to PU's, the data transmission rate in an RBP for PU and SU is the same. This helps to evaluate and compare the data rate at primary user and secondary user[5]. We calculate the achievable data

[5]Note that the sensing algorithm requires two OFDM symbol duration to sense the RBP, hence the overall data rate of SU is lower than PU.

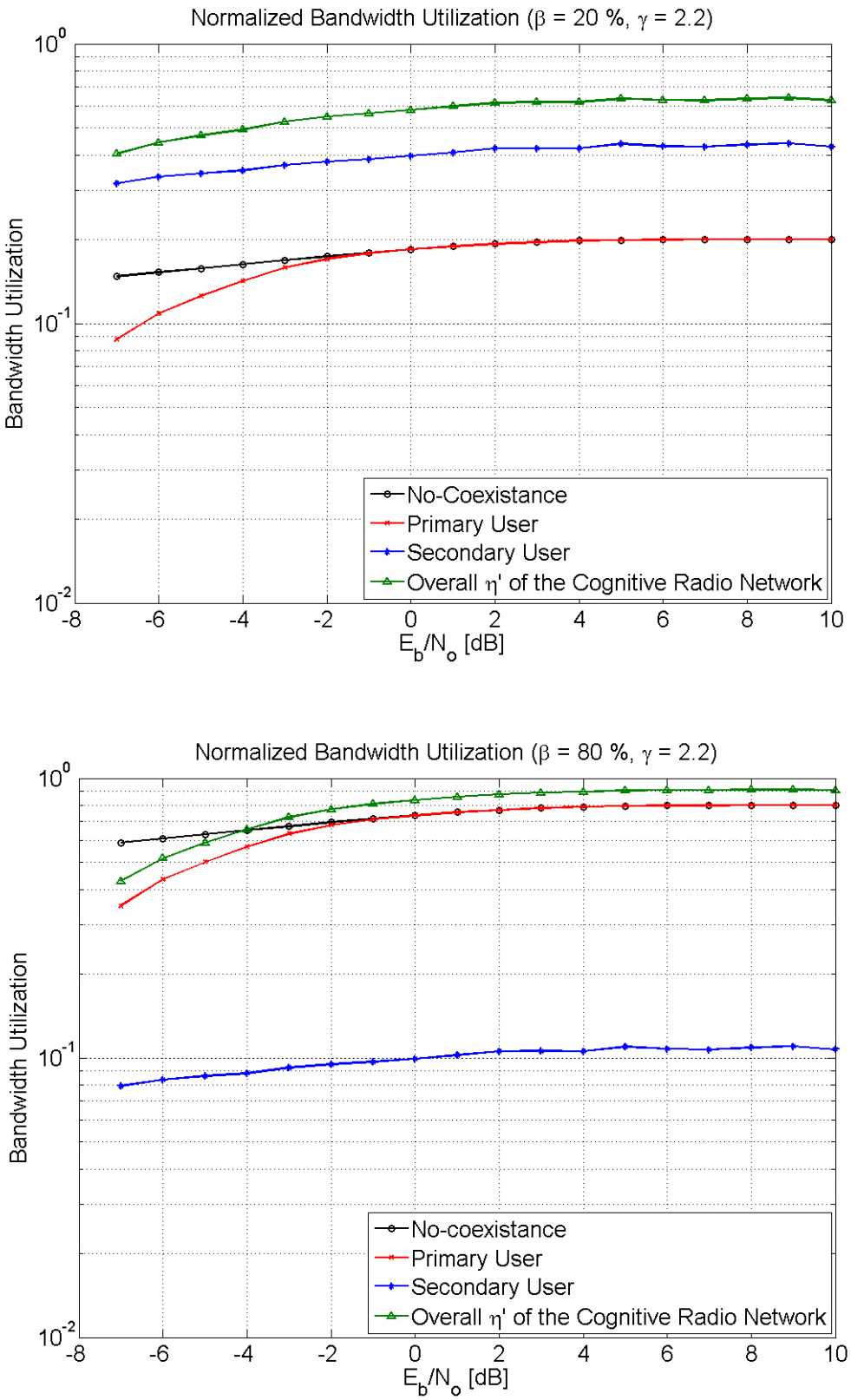

Figure 5.6: Normalized Bandwidth Utilization of the system vs $E_b/N_o[dB]$

rate at secondary user side as a function of primary user activation factor, and the probability of correct detection of an RBP as unused resource. On the other hand, although the algorithm could be configured to achieve a certain amount of accuracy to prevent the interference, the error in spectrum hole detection is inevitable. This causes interference, and hence some data loss for the primary user transmission. We also calculate the data rate lost at the primary user of cognitive radio network. The Normalized bandwidth utilization of the system with respect to primary user activation factor, and the E_b/N_o is considered. It is shown how the activation factor effect the achievable data rate at the secondary user.

Chapter 6

Conclusion and Future Works

6.1 Conclusion

In this thesis, we propose a cognitive scenario where and LTE or LTE-A is the primary user of the system. We develop a combined Cognitive Sensing algorithm, using two main blocks. The first block is obtaining the primary user sub-frame timing, by basically detecting the primary synchronization signal within primary user downlink signal. The second block is the Spectrum Hole Detector which is developed by a fast and accurate frequency domain energy detector. The spectrum hole detector is able to decide on the occupancy of resource block pair in less $350\mu s$ of the beginning of its transmission. The rest of the detected RBP could be used for the transmission of secondary user.

In Chapter 3, we use the detection of PSS within LTE-Downlink signal for obtaining the sub-frame timing of primary user. However, observing and processing all the samples of the received signal is not energy efficient. Therefore, we first recognize the time boundaries of the regions that the PSS may be present. Those boundaries are in fact the OFDM symbol boundaries of the received signal that are obtained by first,

blindly checking whether or not the LTE signal is exist, and secondly identifying it characteristics and finding the OFDM signal parameters. This two-step pre-process is using cyclostationarity properties of OFDM signals. The overall result of the whole process will be the exact time instance that an LTE-Downlink sub-frame starts. This is also the time that channel allocation assignments updates. The probability of miss and false alarm of the PSS detection algorithm is simulated.

In Chapter 4, we propose a multi-step spectrum sensing process, consist of an FFT block, a simple energy detector, and decision making. Unlike a usual LTE receiver, the FFT process is performed on every received OFDM symbol. If the FFT block waits for the whole time slot to be received and then operates, there would be no chance for the SU to transmit as the whole resource is already passed. The timing information from Chapter 3 is used for detecting the energy of the first and/or second ***DATA*** OFDM symbols of each RBP. The calculated energy is compared to a threshold for making the decision on the rest of RBP. Data OFDM symbol follows the control symbols, and if the RBP is not assigned to any primary user these symbols should have no energy. As the scheduling is taken place on every one-millisecond, we simply have a binary hypothesis of zero or one for occupancy of an RBP. The probability of wrong detection of a spectrum hole, which causes interference to the primary user is simulated.

In Chapter 5, we first suggest a transmission scheme which is the best fit for our sensing algorithm. Then we calculate the probability that the SU may produce interference to the primary user. We also calculate the average ***Lost*** data rate of PU transmission due to interference caused by SU. The average amount of data rate that the SU can gain is calculated. Considering QPSK for both PU and SU transmission modulation, and 70 percent activity factor of PU, the PU may lose less that a kbps

while the SU could gain more than 6 Mbps. Note that the amount of data rate loss in PU could be very well controlled by reducing the faults in spectrum hole detection algorithm, and this is one advantage of the system.

6.2 Future Work

As mentioned, the main goal of the presented work, was to show the possibility of such a cognitive scenario where the secondary user is able to exploit the underutilized resources, even if they are only available for less than one-millisecond. The perfectly define specification of LTE was appreciated, as it provides the logic for anticipation of the occupancy of an RBP by only sensing the beginning of it. However, the algorithms and methods that chosen for different section of the proposed Cognitive Sensing process, were the simplest ones. Thus, like any other study, improvements in both performance and the complexity could be seen as the future work.

In addition, the design and implementation of NC-OFDM scheme as secondary user transmission scheme for such a Cognitive Sensing algorithm is a great subject for Future work.

Bibliography

[1] 3GPP. Lte; evolved universal terrestrial radio access (e-utra); physical channel and modulation. Technical Report ETSI TS 136 211, 2014.

[2] Wikipedia Free Encyclopedia. 700 mhz wireless spectrum auction. In *[Online]*. http://en.wikipedia.org/wiki/United_States_2008_wireless_spectrum_auction.

[3] Ericsson. Ericsson mobility report. Technical report, June June 2014.

[4] Federal Communication Commission. Spectrum policy task force report. ET Docket No. 02-135, 2002.

[5] George Lane-Reports Mark A. McHenry, Dan McCloskey. Spectrum occupancy measurements, location 4 of 6: Republican national convention, new york city, ny, aug. 30, 2004sept. 3, 2004, revision 2. Technical report, Shared Spectrum Company, August 2005.

[6] C. E. Shannon. A mathematical theory of communication. *SIGMOBILE Mob. Comput. Commun. Rev.*, 5(1):3–55, January 2001.

[7] J.G. Proakis and M. Salehi. *Digital Communications*. McGraw-Hill International Edition. McGraw-Hill Higher Education, 2008.

[8] B. Sklar. *Digital communications: fundamentals and applications*. Prentice Hall Communications Engineering and Emerging Technologies Series. Prentice-Hall PTR, 2001.

[9] A. Ghosh, J. Zhang, J.G. Andrews, and R. Muhamed. *Fundamentals of LTE*. Prentice Hall Communications Engineering and Emerging Technologies Series. Pearson Education, 2010.

[10] E. Dahlman, S. Parkvall, and J. Sköld. *4G: LTE/LTE-Advanced for Mobile Broadband*. Academic Press. Elsevier/Academic Press, 2011.

[11] Alexander Popescu Westerhagen. *Cognitive Radiio Networks: Elements and Architecture*. PhD thesis, Blekinge Institute of Technology, January 2014.

[12] A.M. Wyglinski, M. Nekovee, and T. Hou. *Cognitive Radio Communications and Networks: Principles and Practice*. Elsevier Science, 2009.

[13] Joseph Mitola III. *Cognitive Radio; An Integrated Agent Architecture for Software Defined Radio*. PhD thesis, KTH/IT/AVH-00/01–SE, 2000.

[14] Cognitive radio for secondary spectrum access (quasar), fp7 strep project, 2010. Fp7 project, Royal Institue of Technology, http://wireless.kth.se/blog/projects/quasar/, 2012.

[15] Simon Haykin. Cognitive radio: brain-empowered wireless communications. *Selected Areas in Communications, IEEE Journal on*, 23(2):201–220, Feb 2005.

[16] Qing Zhao and B.M. Sadler. A survey of dynamic spectrum access. *Signal Processing Magazine, IEEE*, 24(3):79–89, May 2007.

[17] Qing Zhao and A. Swami. A decision-theoretic framework for opportunistic spectrum access. *Wireless Communications, IEEE*, 14(4):14–20, August 2007.

[18] Ning Han, Guanbo Zheng, Sung Hwan Sohn, and Jae Moung Kim. Cyclic autocorrelation based blind ofdm detection and identification for cognitive radio. In *Wireless Communications, Networking and Mobile Computing, 2008. WiCOM '08. 4th International Conference on*, pages 1–5, Oct 2008.

[19] A. Al-Habashna, O.A. Dobre, R. Venkatesan, and D.C. Popescu. Second-order cyclostationarity of mobile wimax and lte ofdm signals and application to spectrum awareness in cognitive radio systems. *Selected Topics in Signal Processing, IEEE Journal of*, 6(1):26–42, Feb 2012.

[20] W. Xu and K. Manolakis. Robust synchronization for 3gpp lte system. In *Global Telecommunications Conference (GLOBECOM 2010), 2010 IEEE*, pages 1–5, Dec 2010.

[21] Zhongshan Zhang, Jian Liu, and Keping Long. Low-complexity cell search with fast pss identification in lte. *Vehicular Technology, IEEE Transactions on*, 61(4):1719–1729, May 2012.

[22] Zhongshan Zhang, Ming Lei, Keping Long, and Yong Fan. Improved cell search and initial synchronization using pss in lte. In *Vehicular Technology Conference (VTC Spring), 2012 IEEE 75th*, pages 1–5, May 2012.

[23] Mai Vu, S.S. Ghassemzadeh, and Vahid Tarokh. Interference in a cognitive network with beacon. In *Wireless Communications and Networking Conference, 2008. WCNC 2008. IEEE*, pages 876–881, March 2008.

[24] F. Shayegh and M.R. Soleymani. Capacity versus interference in ofdm-based cognitive radio systems with beacon. In *Communications (QBSC), 2012 26th Biennial Symposium on*, pages 74–79, May 2012.

[25] W.A. Gardner. *Cyclostationarity in communications and signal processing*. Electrical engineering, communications and signal processing. IEEE Press, 1994.

[26] W.A. Gardner. *Introduction to Random Processes: With Applications to Signals and Systems*. McGraw-Hill, 1990.

[27] Loo Peng Goh, Zhongding Lei, and F. Chin. Dvb detector for cognitive radio. In *Communications, 2007. ICC '07. IEEE International Conference on*, pages 6460–6465, June 2007.

[28] GOH LOO PENG. Study of cyclostationary feature detectors for cognitive radio. Master's thesis, National University of Singapore, 2007.

[29] D. Chu. Polyphase codes with good periodic correlation properties (corresp.). *Information Theory, IEEE Transactions on*, 18(4):531–532, Jul 1972.

[30] M.R. Soleymani and H. Girard. The effect of the frequency offset on the probability of miss in a packet modem using cfar detection method [satellite communication]. *Communications, IEEE Transactions on*, 40(7):1205–1211, Jul 1992.

[31] XILINX. Dsp products introduction. Technical report, XILINX, 2014.

[32] K.S. Hemmert and K.D. Underwood. An analysis of the double-precision floating-point fft on fpgas. In *Field-Programmable Custom Computing Machines, 2005. FCCM 2005. 13th Annual IEEE Symposium on*, pages 171–180, April 2005.

[33] S.M. Kay. *Fundamentals of Statistical Signal Processing: Detection theory*. Prentice Hall Signal Processing Series. Prentice-Hall PTR, 1998.

[34] F.F. Digham, M.-S. Alouini, and Marvin K. Simon. On the energy detection of unknown signals over fading channels. *Communications, IEEE Transactions on*, 55(1):21–24, Jan 2007.

[35] Robert A. Scholtz Moe Z. Win. Impulse radio: How it works. *IEEE COMMUNICATIONS LETTERS*, 2(2), February 1998.

[36] Federal Communications Commission. Fcc first report and order: Revision of part 15 of the commissionss rules regarding ultra-wideband transmission systems. Technical Report ET Docket No. 98-153, April 2002.

[37] K.S. Gilhousen, I.M. Jacobs, R. Padovani, A.J. Viterbi, Jr. Weaver, L.A., and III Wheatley, C.E. On the capacity of a cellular cdma system. *Vehicular Technology, IEEE Transactions on*, 40(2):303–312, May 1991.

[38] Rekha Menon, R.M. Buehrer, and J.H. Reed. Outage probability based comparison of underlay and overlay spectrum sharing techniques. In *New Frontiers in Dynamic Spectrum Access Networks, 2005. DySPAN 2005. 2005 First IEEE International Symposium on*, pages 101–109, Nov 2005.

[39] Jiangzhou Wang and Wong Tat Tung. Narrowband interference suppression in time-hopping impulse radio ultra-wideband communications. *Communications, IEEE Transactions on*, 54(6):1057–1067, June 2006.

[40] C. Rose, Sennur Ulukus, and R.D. Yates. Wireless systems and interference avoidance. *Wireless Communications, IEEE Transactions on*, 1(3):415–428, Jul 2002.

[41] R. Etkin, A. Parekh, and D. Tse. Spectrum sharing for unlicensed bands. *Selected Areas in Communications, IEEE Journal on*, 25(3):517–528, April 2007.

[42] U. Berthold and F.K. Jondral. Guidelines for designing ofdm overlay systems. In *New Frontiers in Dynamic Spectrum Access Networks, 2005. DySPAN 2005. 2005 First IEEE International Symposium on*, pages 626–629, Nov 2005.

[43] T.A. Weiss and F.K. Jondral. Spectrum pooling: an innovative strategy for the enhancement of spectrum efficiency. *Communications Magazine, IEEE*, 42(3):S8–14, Mar 2004.

[44] T. Weiss, J. Hillenbrand, A. Krohn, and F.K. Jondral. Mutual interference in ofdm-based spectrum pooling systems. In *Vehicular Technology Conference, 2004. VTC 2004-Spring. 2004 IEEE 59th*, volume 4, pages 1873–1877 Vol.4, May 2004.

[45] S. Kapoor and S. Nedic. Interference suppression in dmt receivers using windowing. In *Communications, 2000. ICC 2000. 2000 IEEE International Conference on*, volume 2, pages 778–782 vol.2, 2000.

[46] I. Cosovic, S. Brandes, and M. Schnell. A technique for sidelobe suppression in ofdm systems. In *Global Telecommunications Conference, 2005. GLOBECOM '05. IEEE*, volume 1, pages 5 pp.–, Nov 2005.

[47] S. Brandes, I. Cosovic, and M. Schnell. Sidelobe suppression in ofdm systems by insertion of cancellation carriers. In *Vehicular Technology Conference, 2005. VTC-2005-Fall. 2005 IEEE 62nd*, volume 1, pages 152–156, Sept 2005.

[48] R. Rajbanshi, Alexander M. Wyglinski, and G.J. Minden. An efficient implementation of nc-ofdm transceivers for cognitive radios. In *Cognitive Radio Oriented Wireless Networks and Communications, 2006. 1st International Conference on*, pages 1–5, June 2006.

[49] R Rajbanshi. *OFDM-based cognitive radio for DSA networks.* PhD thesis, University of Kansas, Lawrence, KS, USA, May 2007.